Supporting Information

N-confused oxahexaphyrin: oxidative furan ring-opening and fusion triggered chirality

Gaojie Zhu,[a] Zimei Ma,[a] Che Yang,[a] Feng Sha,[a] Glib Baryshnikov,[b] Bin Zhu,[a] Mingbo Zhou,[c] Chengjie Li,[a] Hans Ågren,[d, e] Jianxin Song,[c] Shijun Li,[f] Qizhao Li,*[a] and Yongshu Xie*[a,f]

[a] Shanghai Key Laboratory of Functional Materials Chemistry, Key Laboratory for Advanced Materials and Joint International Research Laboratory of Precision Chemistry and Molecular Engineering, Feringa Nobel Prize Scientist Joint Research Center, Frontiers Science Center for Materiobiology and Dynamic Chemistry, Institute of Fine Chemicals, School of Chemistry and Molecular Engineering, East China University of Science and Technology, Shanghai, 200237, China.

[b] Department of Science and Technology, Laboratory of Organic Electronics, Linköping University, Norrköping, SE-60174, Sweden.

[c] Key Laboratory of Chemical Biology and Traditional Chinese Medicine, Ministry of Educational of China, Key Laboratory of the Assembly and Application of Organic Functional Molecules of Hunan Province College of Chemistry and Chemical Engineering, Hunan Normal University, Changsha 410081, China

[d] Department of Physics and Astronomy, Uppsala University, SE-751 20 Uppsala, Sweden.

[e] Faculty of Chemistry, Wroclaw University of Science and Technology, Wyb. Wyspianskiego 27, PL-50370 Wroclaw, Poland.

[f] College of Material, Chemistry and Chemical Engineering, Hangzhou Normal University, Hangzhou, 311121, Zhejiang, China

*E-mail: yshxie@ecust.edu.cn; zhaolq@ecust.edu.cn.

Table of Contents

1. Experimental Information

General

Commercially available solvents and reagents were used without further purification unless otherwise mentioned. Thin-layer chromatography (TLC) was carried out on glass sheets coated with silica gel 60 GF254 (XINNUO Chemical Co., Ltd.). NMR spectra were recorded using Bruker AM 400/600 or Varian 400-MR spectrometers. The chemical shifts were calibrated using $CDCl_3$ (δ = 7.26 ppm) as internal standards for ^1H NMR, ^1H, ^1H-COSY and ^1H, ^1H-NOESY; and using $CDCl_3$ (δ = 77.16 ppm) as internal standards for ^{13}C NMR spectra. HRMS were collected using various spectrometers including Waters Xevo G2-XS QTof, Aglient 7250 & JEOL-JMS-T100LP Accu TOF and Thermo Scientific Q Exactive quadrupole-Orbitrap mass spectrometers. UV-Vis-NIR absorption spectra were recorded on Shimadzu UV-3600 spectrophotometer at room temperature. The HPLC analyses were performed on Shimadzu LC-16P. Chiralpak IA column was purchased from Daicel Chiral Technologies. Circular dichroism (CD) spectra were measured with JASCO J-1500 spectrometer.

Crystallography

X-ray analyses were performed on a SMART APEX equipped with CCD detectors (Bruker) using CuK\a (graphite, monochromated, λ = 1.54178 Å) and MoKα (graphite, monochromated, λ = 0.71073 Å). The structures were solved by the direct methods of SHELXS-97 and refined using the SHELXL-2015 programs.[S1-S3] The positional parameters and thermal parameters of non-hydrogen atoms were refined anisotropically on F^2 by the full-matrix least-squares method. Hydrogen atoms were placed at calculated positions and refined riding on their corresponding carbon atoms. Single crystals of **2-Br** were obtained by the slow recrystallization from the dichloromethane/n-hexane solution, and the crystals of **3** were obtained by the slow evaporation from the chloromethane/n-heptane solution. **2-Br** (CCDC: 2466477) and **3** (CCDC: 2466476) contain the supplementary crystallographic data for this paper. These data can be obtained free of charge from The Cambridge Crystallographic Data Centre via *www.ccdc.cam.ac.uk/data_request/cif.*

Electrochemical Measurements

Cyclic voltammetry (CV) and differential pulse voltammetry (DPV) studies were carried out on a CorrTest Instrument Model CS350H with electrochemical system utilizing the three-electrode method consisting of a platinum wire (working electrode), platinum ring (counter electrode) and Ag/AgCl (reference electrode) in dry CH_2Cl_2 with $TBAPF_6$ as the electrolyte and ferrocene as external standard. Absolute CH_2Cl_2 was purchased from Macklin and used as received and $TBAPF_6$ was purchased from Fluka Chemika, and recrystallized from ethanol and vacuum dried at 40 °C for at least one week prior to use.

Details for Theoretical Calculations.

Density functional theory (DFT) calculations were carried out using the Gaussian 16 program. The optimized structures, relative energies, and molecular orbitals were all calculated at the level of B3LYP,[S4, S5] employing a basis set 6-31G for all atoms. The nucleus-independent chemical shift (NICS) calculations were obtained using the GIAO method at the B3LYP/6-31G level.[S6] The local ring center chosen for determination of the NICS values[S7] represent the nonweighted means of the carbon and nitrogen coordinates on the peripheral positions of the macrocycles. ACID contours with the associated vectors were obtained in accord with the continuous set of gauge transformation (CSGT) methods[S8a] and at the same computational level used to obtain the optimized geometries.

At the optimized geometries, time-dependent (TD) DFT calculations with the hybrid PBE0 functional[S8b] were carried out to simulate the absorption spectra.

2. Experimental procedures

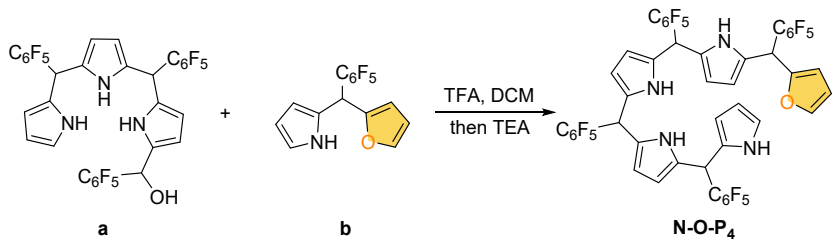

a **b** **N-O-P$_4$**

Synthesis of **N-O-P$_4$**: Tripyrrane monocarbinol **a** (1.20 g, 1.59 mmol) and oxa-dipyrromathane **b** (1.99 g, 6.37 mmol) were dissolved in CH_2Cl_2 (100 mL). After the solution was stirred for 15 min, TFA (60 μL, 0.79 mmol) was then added and the mixture was further stirred at room temperature for 4 h in the dark. The reaction was quenched by addition of Et_3N (113 μL, 0.82 mmol) and then evaporated in vacuo. The crude residue was separated by chromatography on a silica gel column with petroleum ether/CH_2Cl_2 (7/3–1/1, v/v) solutions used as the eluents, affording excessive **b** as the first eluted fraction and **N-O-P$_4$** as the second fraction afforded (683 mg, 41%). ^{1}H NMR (400 MHz, $CDCl_3$, ppm): δ = 8.32 (s, 1H, NH), 8.19 (s, 1H, NH), 8.09 (s, 2H, NH), 7.34 (s, 1H), 6.72 (t, J = 2.2 Hz, 1H), 6.33 (t, J = 2.6 Hz, 1H), 6.14 (d, J = 2.9 Hz, 1H), 6.08 (d, J = 3.4 Hz, 1H), 5.98 – 5.96 (m, 2H), 5.91 – 5.86 (m,5H), 5.82 – 5.74 (m, 4H). ^{19}F NMR (376 MHz, $CDCl_3$, ppm): δ = −141.73 – −142.25 (m, 6F), −142.28 – −142.48 (m, 2F), −155.86 – −155.20 (m, 3F), −155.22 – −155.43 (m, 1F), −160.72 – −161.16 (m, 6F), −161.31 (ddt, J = 26.5, 12.7, 6.5 Hz, 2F). HRMS: *m/z*; $[M-H]^-$, calcd for: $C_{48}H_{19}F_{20}N_4O$: 1047.1240; found: 1047.1245.

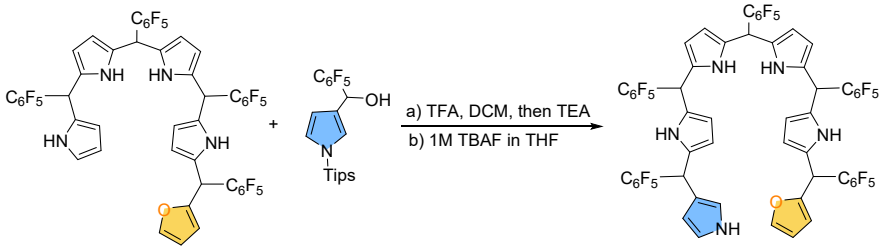

N-O-P$_4$ **N-O-P$_5$**

Synthesis of **N-O-P$_5$**: A solution of **N-O-P$_4$** (600 mg, 0.572 mmol) and Tips-pyrrole-β-carbinol (360 mg, 0.858 mmol) in CH_2Cl_2 (60 mL) was stirred for 10 min at room temperature, and then TFA (22 μL, 0.28 mmol) was added and the solution was further stirred at room temperature for 6 h. After adding Et_3N (42 μL, 0.30 mmol), the solvent was evaporated in vacuo. The residue was dissolved in THF, and TBAF (0.60 mL, 0.60 mmol, 1.0 M in THF) was added slowly for 5 min. The resulting mixture was stirred for 1 h. After the deprotection was complete (monitored with TLC), the reaction was quenched with water, and CH_2Cl_2 was added. Then the organic layer was separated, washed twice with brine and dried over Na_2SO_4. Removal of the solvent followed by

silica gel column chromatography with CH_2Cl_2/ petroleum ether (1/1, v/v) afforded **N-O-P$_5$** as a white solid (473 mg, 64%, two steps). ^{1}H NMR (400 MHz, $CDCl_3$, ppm): δ = 8.28 (s, 1H, NH), 8.20 – 8.10 (m, 2H, NH), 8.00 (d, J = 10.6 Hz, 2H, NH), 7.34 – 7.32 (m, 1H), 6.75 – 6.73 (m, 1H), 6.58 – 6.56 (m, 1H), 6.33 (s, 1H), 6.07 (d, J = 3.2 Hz, 2H), 5.97 (s, 1H), 5.93 – 5.87 (m, 7H), 5.80 (s, 1H), 5.78 (s, 1H), 5.75 (d, J = 7.6, 3H). ^{13}C NMR (101 MHz, $CDCl_3$, ppm): δ = 151.3, 146.1, 143.6, 142.4, 139.0, 136.5, 131.3, 128.8, 128.5, 127.9, 127.4, 126.6, 121.1 (t, ^2J = 18 Hz*), 118.8, 116.3, 115.9 (d, ^1J = 344 Hz*), 110.6, 108.2, 108.0, 107.8, 107.6, 106.9. (*These signals showed further long-range coupling with the fluorine atoms and would be less accurate). HRMS: *m/z*; [*M*+H]$^+$, calcd for: $C_{59}H_{25}F_{25}N_5O$: 1294.1660; found: 1294.1651.

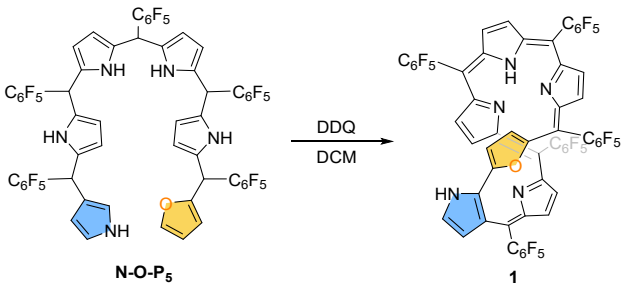

N-O-P$_5$ **1**

Synthesis of **1**: A sample of **N-O-P$_5$** (1.20 g, 0.928 mmol) was dissolved in CH_2Cl_2 (1 L), then a solution of DDQ (1.05 g, 4.64 mmol) in CH_2Cl_2 (200 mL) was slowly added to the stirred mixture. The mixture was then stirred for an additional 2 h, and the reaction was quenched with water, and washed with brine for three times. The organic phase was dried over Na_2SO_4 and evaporated in *vacuo*. The residue was purified by silica gel column chromatography using petroleum ether/dichloromethane = 4/1 (v/v) as the eluent to obtain **1** as red-colored solid (548 mg, 46%). ^{1}H NMR (400 MHz, $CDCl_3$, ppm): δ = 14.66 (s, 1H, NH), 13.86 (s, 1H, NH), 7.97 (s, 1H), 7.85 (d, J = 6.0 Hz, 1H), 6.84 (d, J = 5.6 Hz, 1H), 6.74 (d, J = 13.6 Hz, 1H), 6.53 (d, J = 4.8 Hz, 1H), 6.43 (d, J = 13.2 Hz, 1H), 6.37 (s, 1H), 6.32 (d, J = 5.6 Hz, 1H), 6.18 (s, 1H), 6.10 (d, J = 4.8 Hz, 1H), 6.02 (d, J = 7.2 Hz, 2H). ^{19}F NMR (376 MHz, $CDCl_3$, ppm): δ = 129.10 (d, J = 25.4 Hz, 1F), −136.18 – −136.30 (m, 1F), −136.70 (d, J = 25.4 Hz, 1F), −136.83 (d, J = 20.4 Hz, 1F), −137.03 (d, J = 22.9 Hz, 1F), −137.62 (d, J = 25.4 Hz, 1F), −137.79 (d, J = 22.9 Hz, 1F), −137.92 (d, J = 22.9 Hz, 1F), −140.41 (dd, J = 61.0 Hz, 22.9 Hz, 1F), −142.72 (d, J = 25.4 Hz, 1F), −148.57 (1F), −151.01 (dt, J = 58.5, 21.6 Hz, 2F), −152.26 (t, J = 21.6 Hz, 1F), -153.23(t, J = 21.6 Hz, 1F), −158.56 (d, J = 22.9 Hz, 2F), −159.68 (t, J = 22.9 Hz, 1F), −159.85 (t, J = 21.6 Hz, 1F), −160.16 – −160.30 (m, 3F), −160.64 (t, J = 22.9 Hz, 2F), −162.19 (d, J = 25.4 Hz, 1F). UV/Vis/NIR [(CH_2Cl_2): λ_{max} (nm) (ε/10^5 mol^{-1}dm^{3}cm^{-1})]: 360 (0.28), 442 (0.29), 543 (0.28), 685–1200 (broad peak). HRMS: *m/z*; [*M*+H]$^+$, calcd for: $C_{59}H_{15}F_{25}N_5O$: 1284.0877; found: 1284.0865.

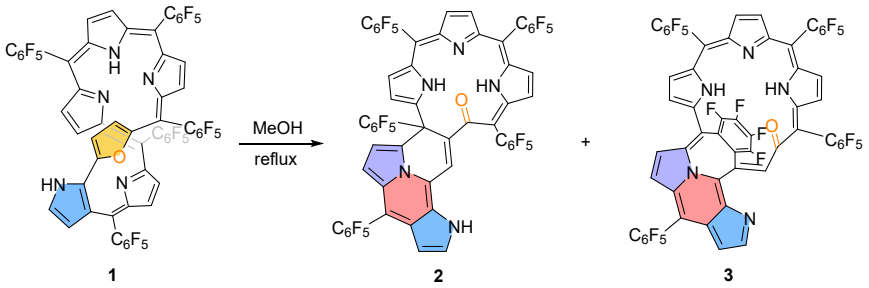

Synthesis of **2** and **3**: A sample of **1** (120 mg, 0.0935 mmol) was dissolved in MeOH (20 mL), and the solution was stirred at reflux overnight. After cooling to room temperature, water was added to quench the reaction. The organic phase was evaporated in *vacuo*. The crude residue was purified by silica gel column chromatography using petroleum ether/dichloromethane = 4/1 (v/v) as the eluent first to obtain **2** as a green solid (27.6 mg, 23%) and then petroleum ether/ethyl acetate = 3/1 (v/v) was used as the eluent to obtain **3** as a red solid (33.1 mg, 28%).

2: ^{1}H NMR (600 MHz, $CDCl_3$, ppm): δ = 12.99 (s, 1H, NH), 10.41 (s, 1H, NH), 8.00 (s, 1H, NH), 7.23 (s, 1H), 7.17 (d, J = 3.6 Hz, 1H), 6.67 (d, J = 4.2 Hz, 2H), 6.61 (d, J = 5.4 Hz, 1H), 6.55 (d, J = 4.2 Hz, 1H), 6.39 (d, J = 4.2 Hz, 1H), 6.28 (d, J = 4.8 Hz, 1H), 6.10 – 6.08 (m, 2H), 5.33 – 5.22 (m, 1H). ^{13}C NMR (151 MHz, $CDCl_3$, ppm): δ = 196.0, 167.8, 151.7, 150.6, 150.0, 149.2, 144.9 (d, $^{1}J_{CF}$ = 251 Hz*), 138.0 (d, $^{1}J_{CF}$ = 257 Hz*), 134.7, 133.4, 133.0, 131.3, 131.2, 130.1, 129.8, 128.4, 128.3, 126.8, 125.6, 121.7, 118.8, 118.4, 115.1, 114.9, 113.4, 112.8, 110.9 (t, $^{2}J_{CF}$ = 60 Hz*), 102.8, 102.6, 99.9, 95.4, 60.4. (*These signals showed further long-range coupling with the fluorine atoms and would be less accurate). UV/Vis/NIR [(CH_2Cl_2): λ_{max} (nm) ($\varepsilon/10^5$ $mol^{-1}dm^3cm^{-1}$)]: 376 (0.35), 425 (0.26), 638 (0.21), 700–1000 (broad peak). HRMS: *m/z*; $[M+H]^+$, calcd for: $C_{59}H_{15}F_{25}N_5O$: 1284.0877; found: 1284.0879.

3: ^{1}H NMR (600 MHz, $CDCl_3$, ppm): δ = 13.22 (s, 1H, NH), 11.40 (s, 1H, NH), 8.40 (d, J = 1.2 Hz, 1H), 7.51 (d, J = 6.0 Hz, 1H), 6.89 (s, 1H), 6.86 (d, J = 6.0 Hz, 1H), 6.80 (dd, J = 4.2 Hz, 1.8 Hz, 1H), 6.69 (d, J = 4.8 Hz, 1H), 6.61 (d, J = 5.4 Hz, 1H), 6.51 (s, 2H), 6.47 (d, J = 5.4 Hz, 1H), 6.29 (d, J = 4.8 Hz, 1H). ^{13}C NMR (151 MHz, $CDCl_3$, ppm): δ = 166.81, 159.59, 156.58, 152.61, 146.69, 144.82 (d, $^{1}J_{CF}$ = 250 Hz*), 143.02 (t, $^{2}J_{CF}$ = 42 Hz*), 142.65, 141.34, 139.46, 138.29, 137.99, 137.28, 136.80, 136.68, 133.76, 131.72, 131.05, 129.39, 128.23, 126.41, 126.34, 124.93, 123.06, 115.93, 108.84, 107.70, 105.67, 96.56. (*These signals showed further long-range coupling with the fluorine atoms and would be less accurate). ^{19}F NMR (376 MHz, , $CDCl_3$, ppm): δ = −136.73 (dd, J = 24.5, 6.8 Hz, 2F), −137.55 (dd, J = 23.8, 8.9 Hz, 2F), −138.16 (dd, J = 23.8, 7.5 Hz, 2F), −138.30 – −138.47 (m, 2F), −139.14 – −139.22 (m, 1F), −143.79 (d, J = 12.3 Hz, 1F), −150.96 – −151.25 (m, 3F), −151.52 – −151.72 (m, 2F), −153.01 (t, J = 19.8 Hz, 1F), −158.57 – −158.72 (m, 1F), −159.81 – −160.18 (m, 4F), −160.35 (td, J = 23.2, 22.5, 8.9 Hz, 1F), −160.64 (ddt, J = 21.8, 16.3, 8.2 Hz, 2F). UV/Vis/NIR [(CH_2Cl_2): λ_{max} (nm) ($\varepsilon/10^5$ $mol^{-1}dm^3cm^{-1}$)]: 405 (0.40),

514 (0.44), 724 (0.10). HRMS: *m/z*; $[M+H]^+$, calcd for: $C_{59}H_{14}F_{24}N_5O$: 1264.0815; found: 1264.0813.

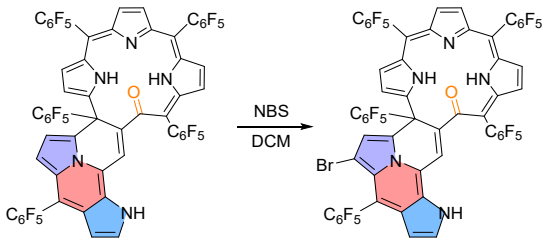

Synthesis of **2-Br**: NBS (3.6 mg, 0.020 mmol) was dissolved in CH_2Cl_2 (5 mL) and slowly added into the solution of **2** (25 mg, 0.020 mmol) in CH_2Cl_2 (10 mL). The solution was stirred at room temperature for 10 minutes, and quenched with water. The organic phase was washed with water, dried with anhydrous Na_2SO_4, and the solvent was removed in vacuo. The residue was separated through silica gel column chromatography using PE/EA = 7/1 (v/v) as the eluent, yielding a green product of **2-Br** (23 mg, 88%). ^{1}H NMR (400 MHz, $CDCl_3$, ppm): δ 12.94 (s, 1H, NH), 10.32 (s, 1H, NH), 8.06 (s, 1H, NH), 7.19 (s, 2H), 6.68 (d, J = 4.8 Hz, 2H), 6.62 (d, J = 5.6 Hz, 1H), 6.57 (s, 1H), 6.29 (d, J = 4.4 Hz, 1H), 6.12 (s, 1H), 6.03 (s, 1H), 5.38 (dd, J = 1.6 Hz, 4.0 Hz, 1H). ^{13}C NMR (151 MHz, $CDCl_3$, ppm): δ = 196.14, 167.95, 150.76, 150.41, 150.16, 149.23, 145.02 (d, $^1J_{CF}$ = 251 Hz*), 137.63 (d, $^1J_{CF}$ = 254 Hz*), 134.79, 133.29, 133.09, 131.33, 131.17, 130.77, 128.47, 128.07, 127.47, 126.94, 125.51, 121.75, 118.88, 117.88, 117.67, 113.97, 113.40, 113.32, 102.35, 99.53, 88.84, 60.39. (*These signals showed further long-range coupling with the fluorine atoms and would be less accurate). HRMS: *m/z*; $[M+H]^+$, calcd for: $C_{59}H_{14}BrF_{25}N_5O$: 1361.9983, found: 1361.9969.

Table S1 Yields of compounds **1** and **2** obtained under various conditions.

Entry	Temperature(°C)	Time (h)	Solvent	Yield of **2**	Yield of **3**
1	r.t	12	MeOH	--	--
2	r.t	72	MeOH	--	--
3	65	12	MeOH	23%	28%
4	r.t	12	THF	<1%	--
5	r.t	72	THF	<1%	--
6	65	12	THF	12%	<1%
7	r.t	12	MeCN	<1%	--
8	r.t	72	MeCN	<1%	<1%
9	65	12	MeCN	11%	5%
10	r.t	12	Toluene	--	--
11	r.t	72	Toluene	<1%	<1%
12	65	12	Toluene	14%	17%
13	r.t	12	DMF	--	--
14	r.t	72	DMF	<1%	--
15	65	12	DMF	15%	<1%

3. NMR Spectra

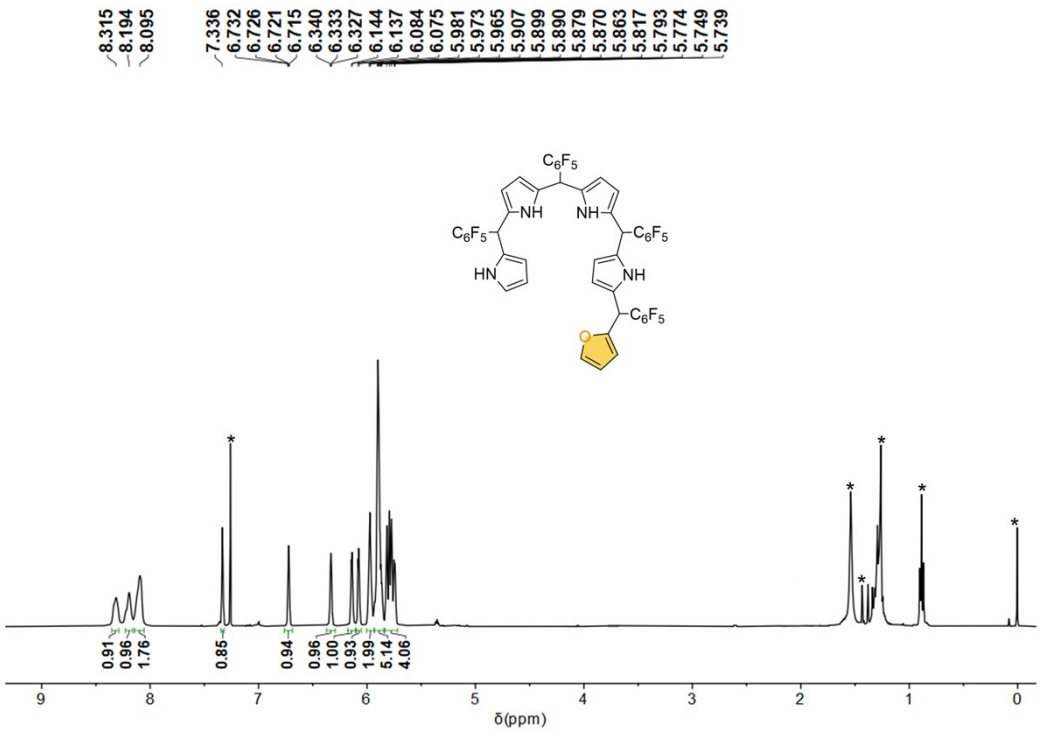

Figure S1. ^{1}H NMR (400 MHz) spectrum of **N-O-P$_4$** in $CDCl_3$.

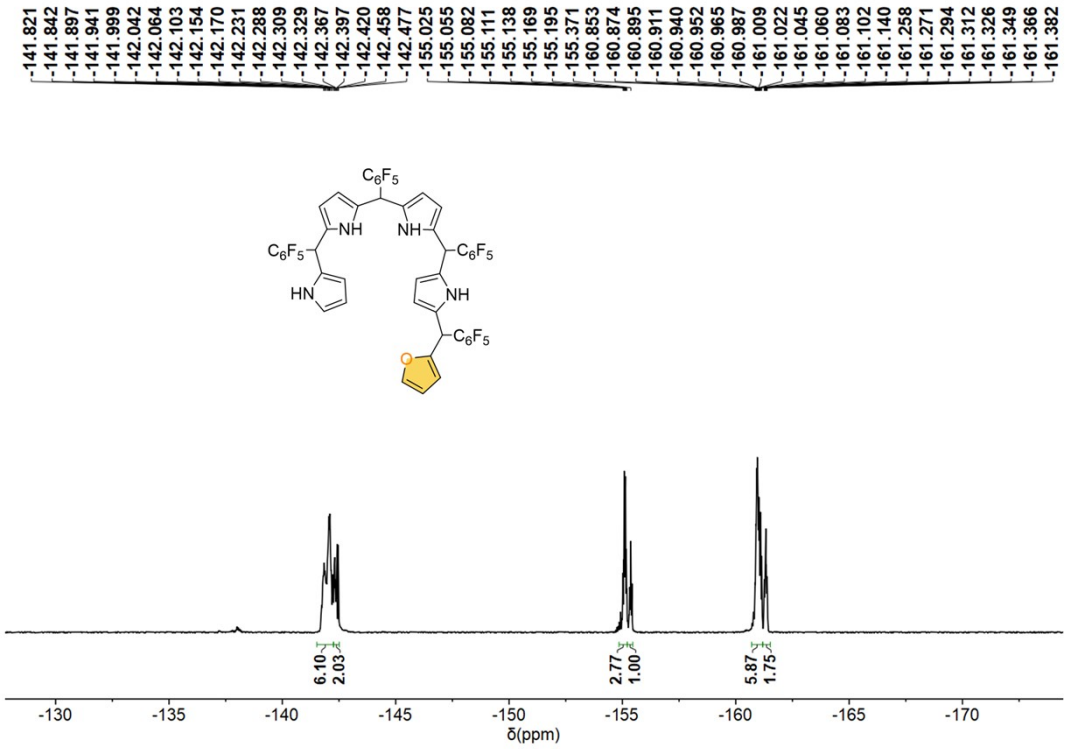

Figure S2. ^{19}F NMR (376 MHz) spectrum of **N-O-P$_4$** in $CDCl_3$.

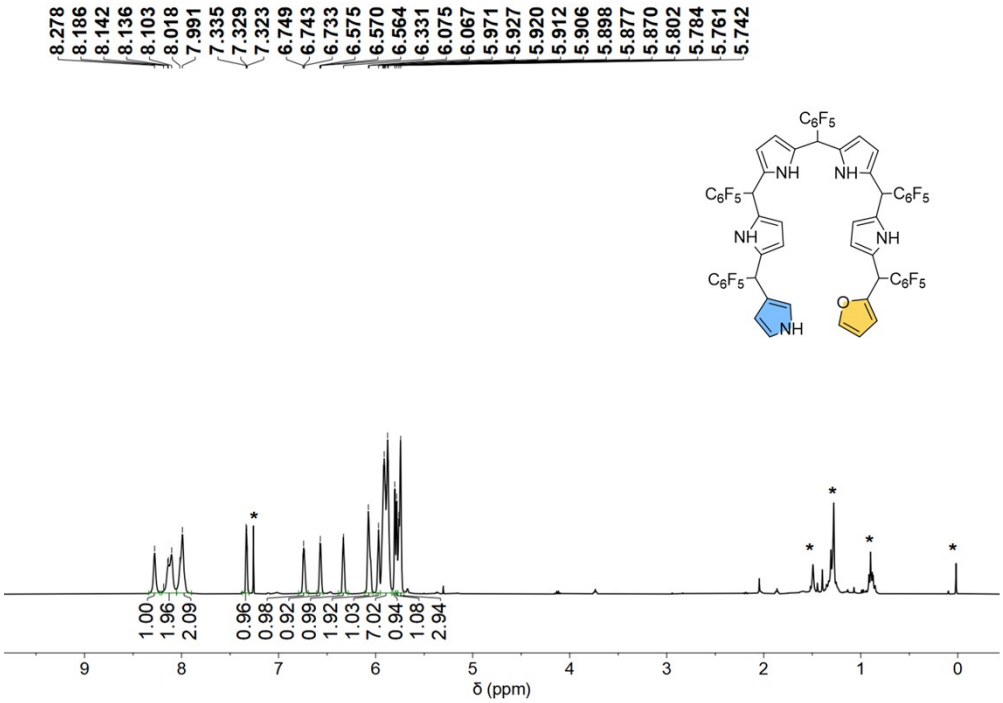

Figure S3. ^{1}H NMR (400 MHz) spectrum of **N-O-P$_5$** in $CDCl_3$.

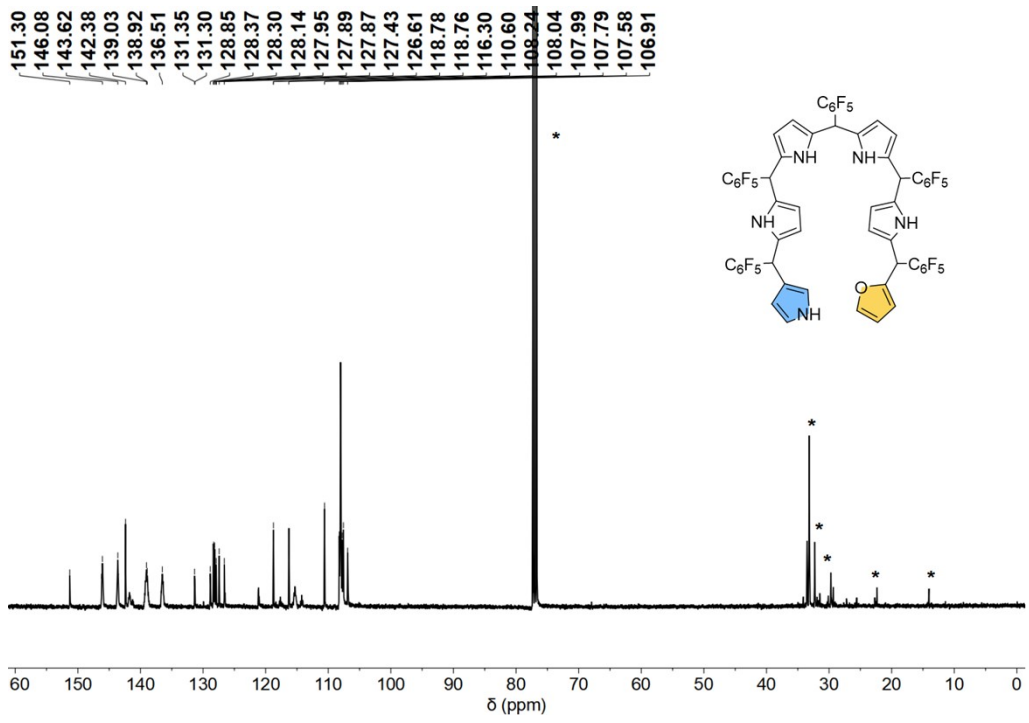

Figure S4. ^{13}C NMR (101 MHz) spectrum of **N-O-P$_5$** in $CDCl_3$.

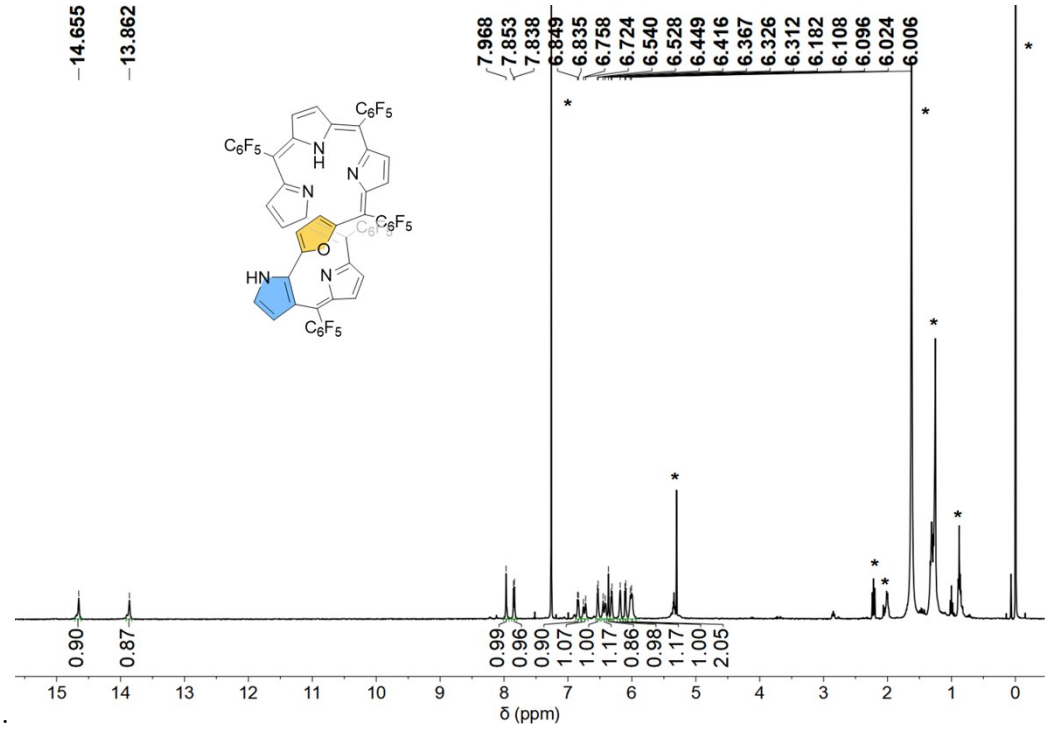

Figure S5. ^{1}H NMR (400 MHz) spectrum of **1** in $CDCl_3$.

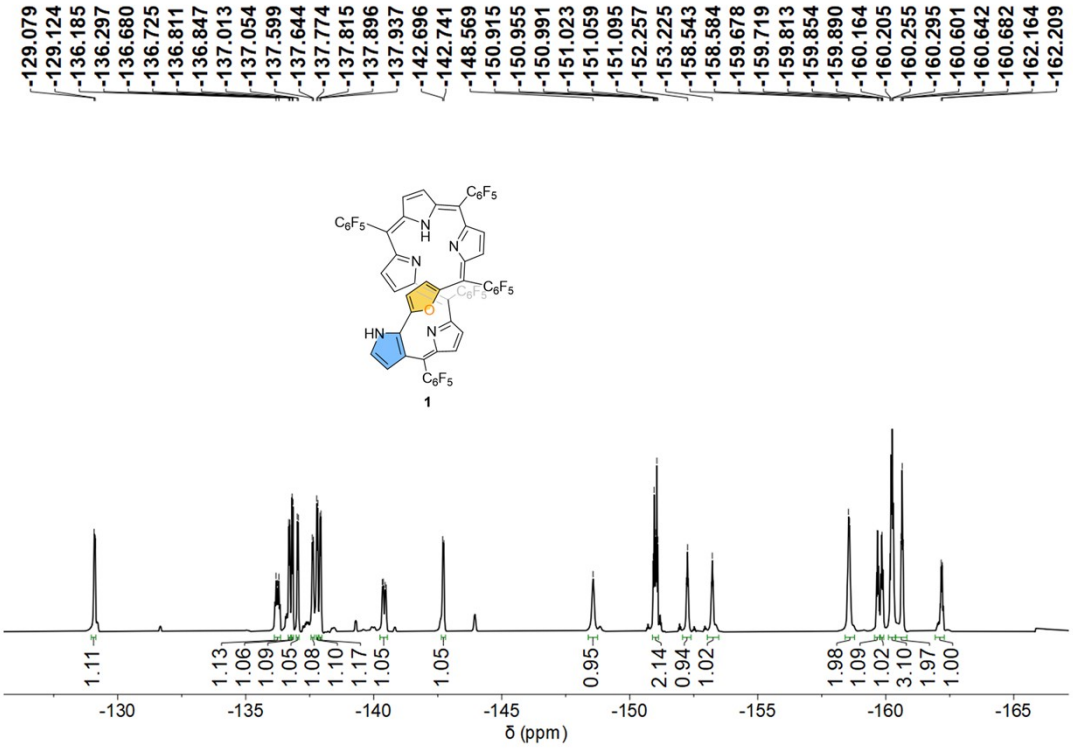

Figure S6. ^{19}F NMR (376 MHz) spectrum of **1** in $CDCl_3$.

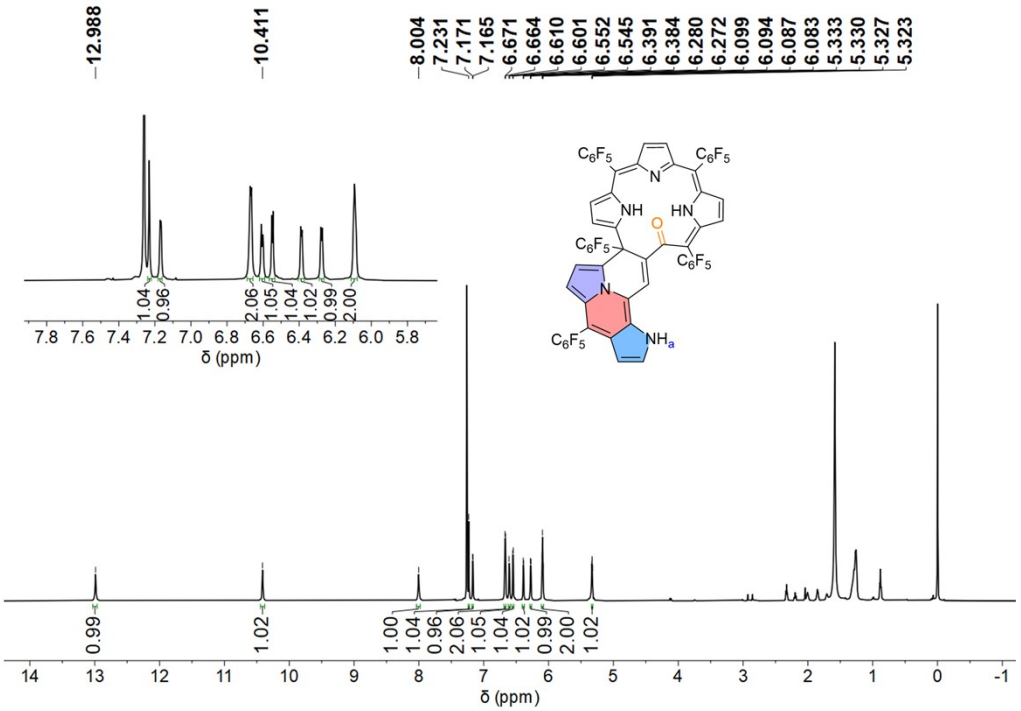

Figure S7. ^{1}H NMR (400 MHz) spectrum of **2** in $CDCl_3$.

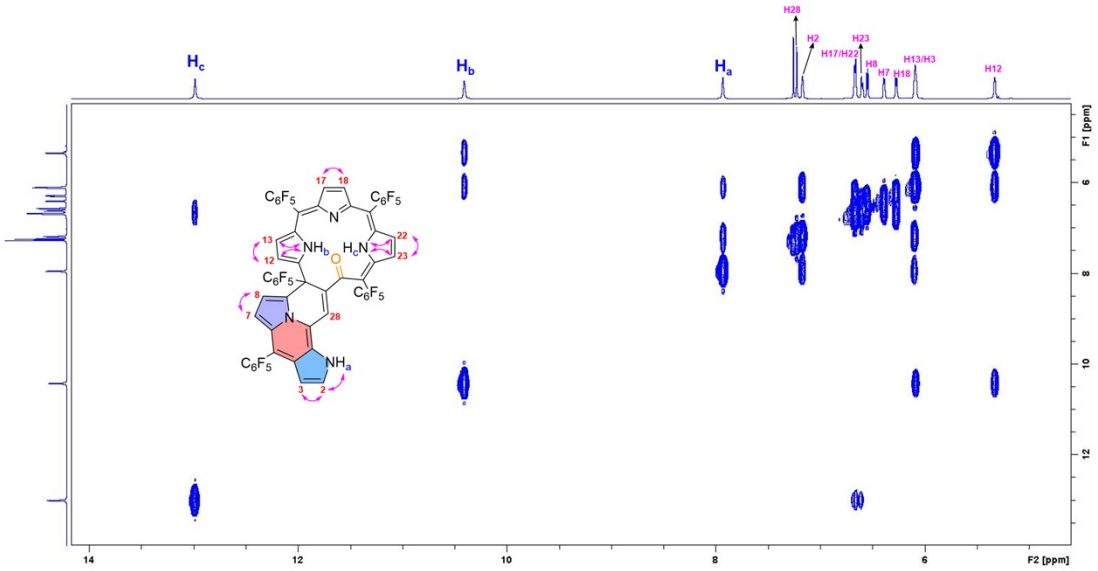

Figure S8. ^{1}H-^{1}H COSY NMR (400 MHz) spectrum of **2** in $CDCl_3$.

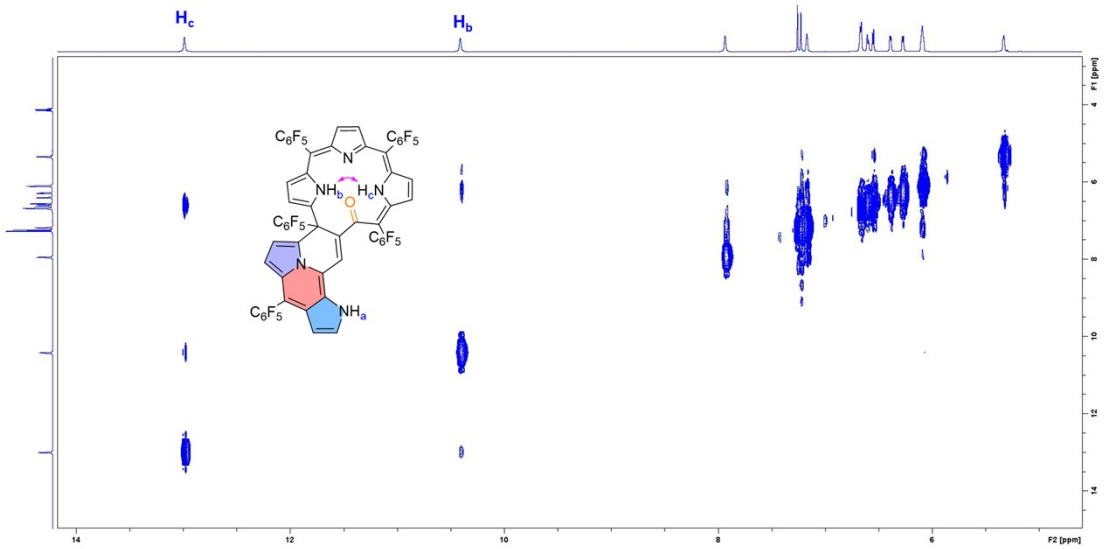

Figure S9. ^{1}H-^{1}H ROESY NMR (400 MHz) spectrum of **2** in $CDCl_3$.

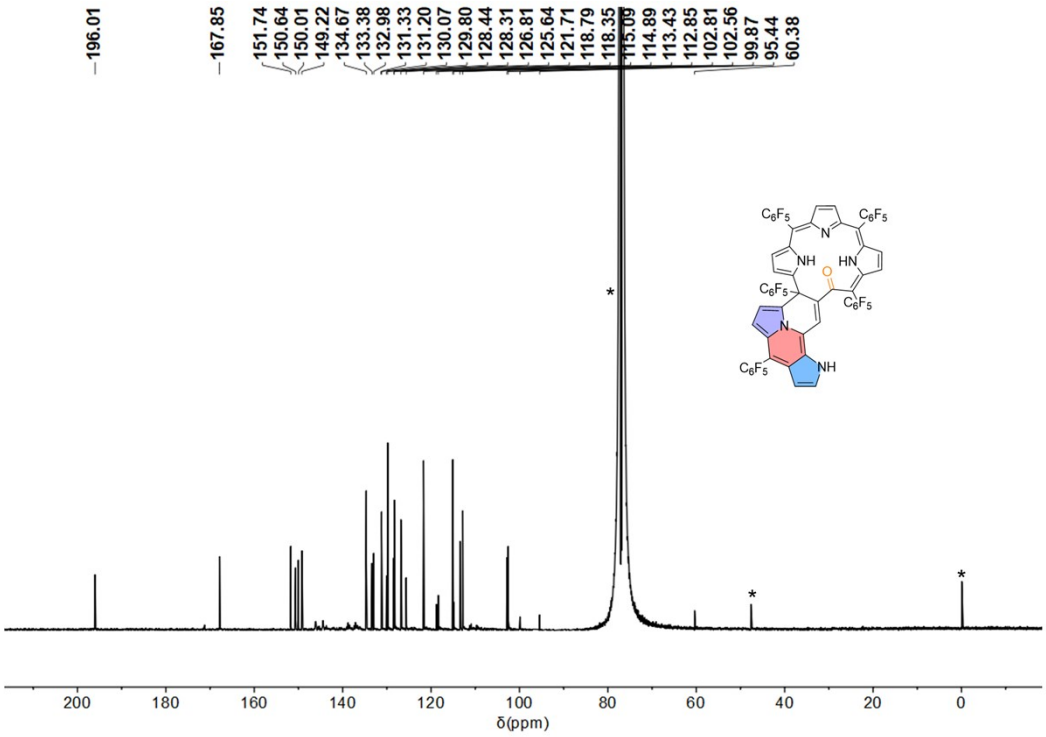

Figure S10. ^{13}C NMR (151 MHz) spectrum of **2** in $CDCl_3$.

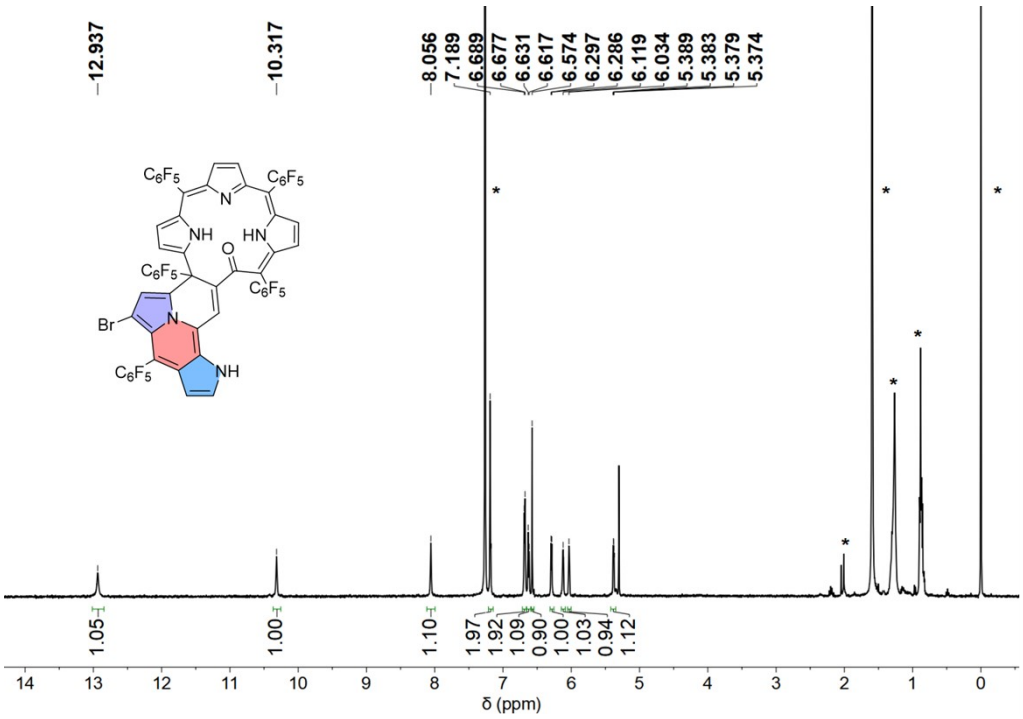

Figure S11. ^{1}H NMR (400 MHz) spectrum of **2-Br** in $CDCl_3$.

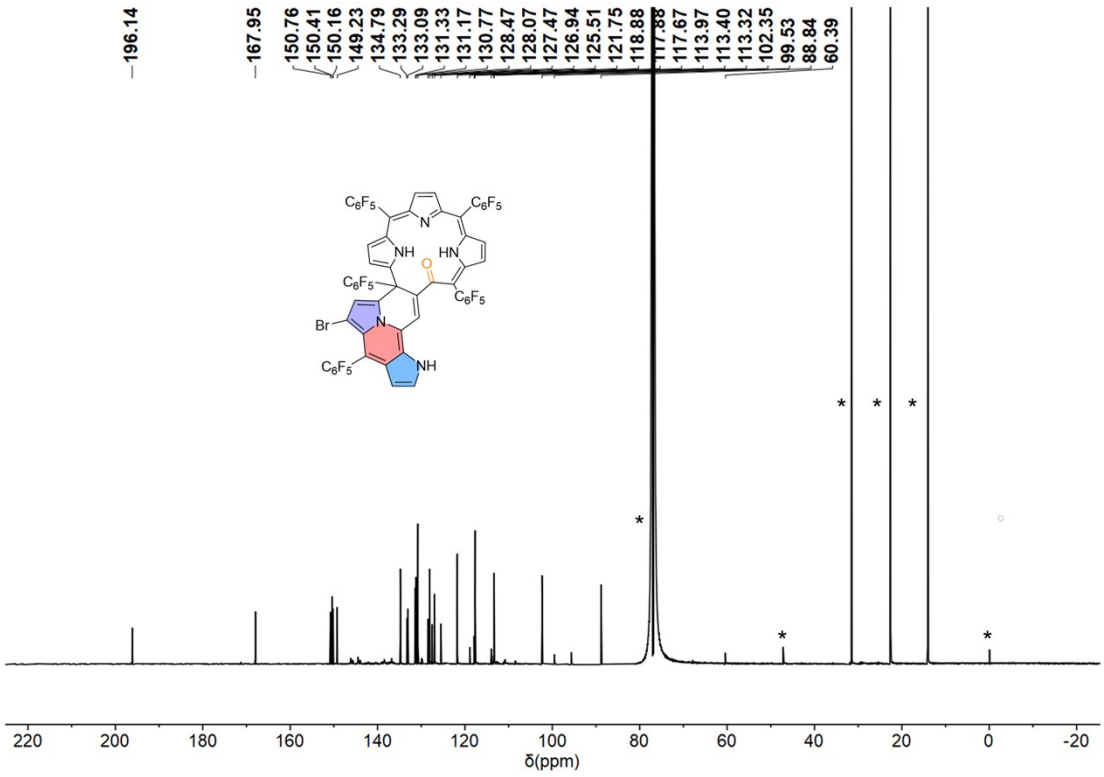

Figure S12. ^{13}C NMR (151 MHz) spectrum of **2-Br** in $CDCl_3$.

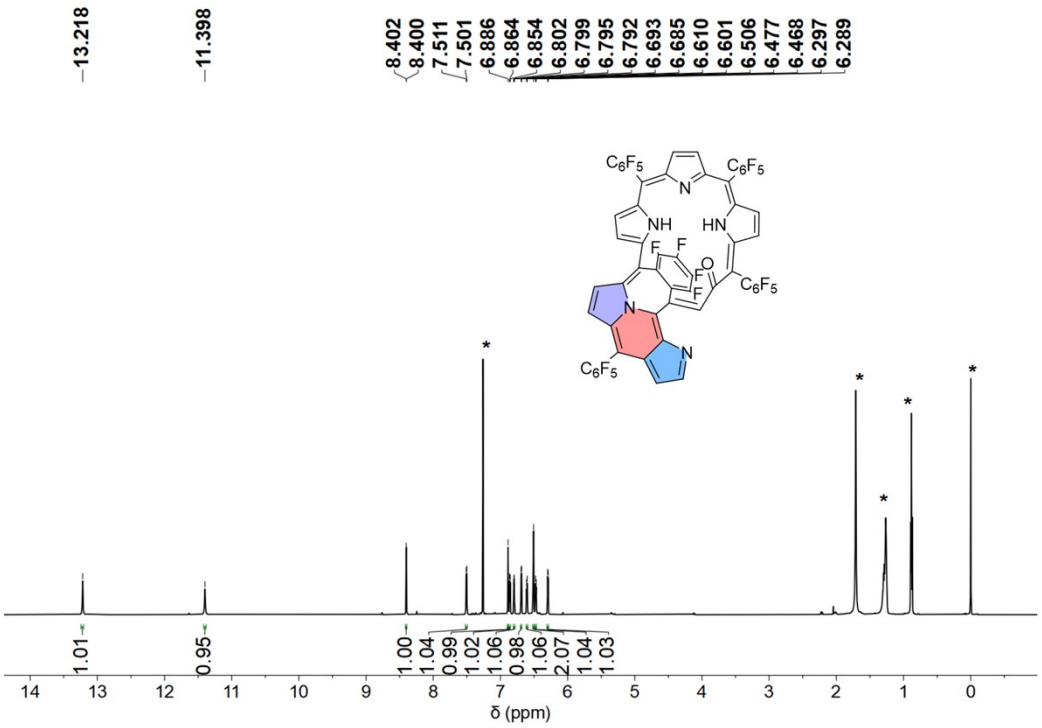

Figure S13. ^{1}H NMR (400 MHz) spectrum of **3** in $CDCl_3$.

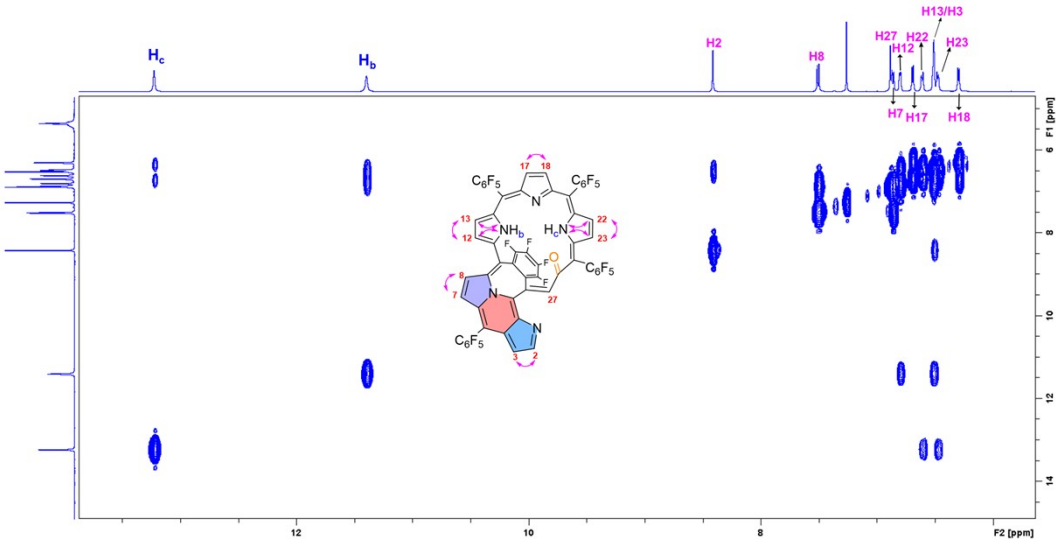

Figure S14. ^{1}H-^{1}H COSY NMR (400 MHz) spectrum of **3** in $CDCl_3$.

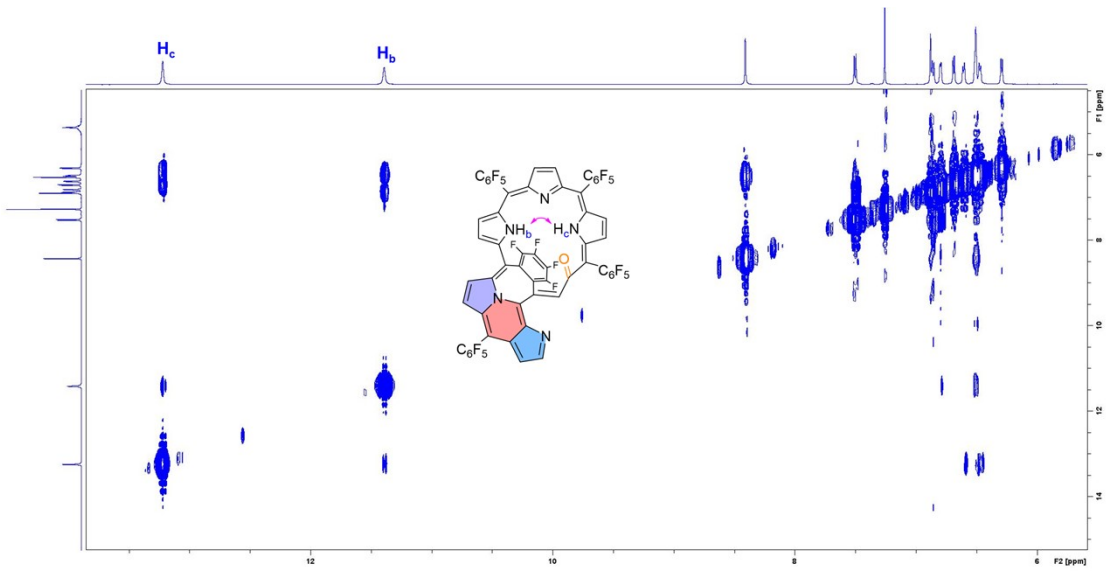

Figure S15. ^{1}H-^{1}H ROSY NMR (400 MHz) spectrum of **3** in $CDCl_3$.

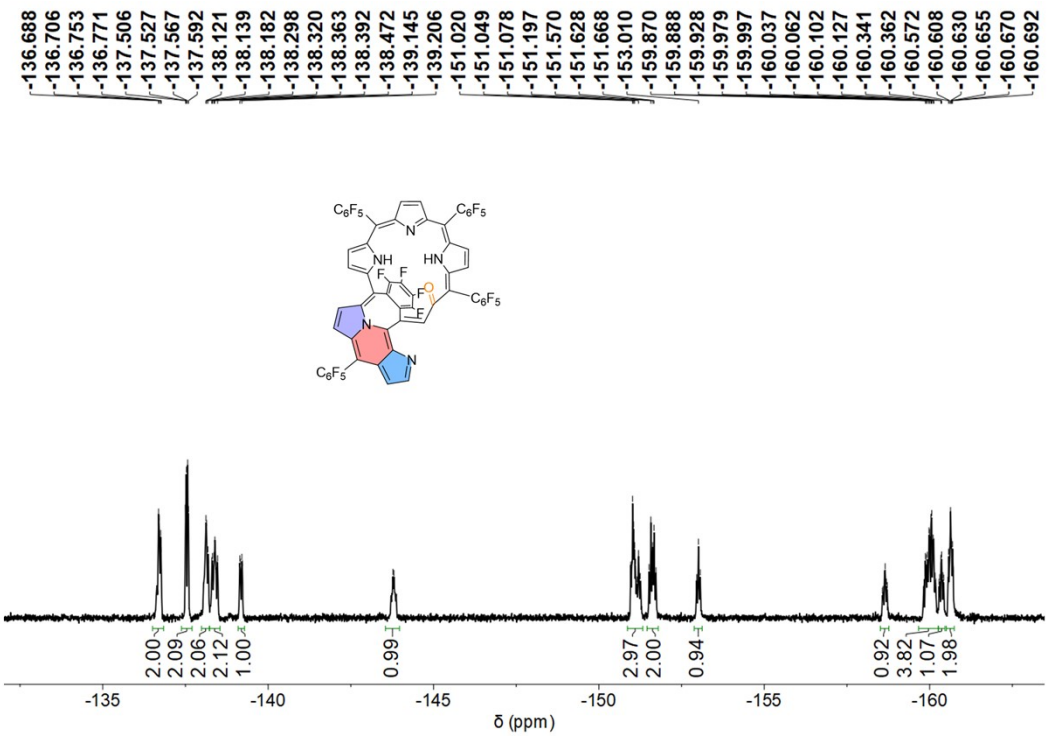

Figure S16. ^{19}F NMR (376 MHz) spectrum of **3** in $CDCl_3$.

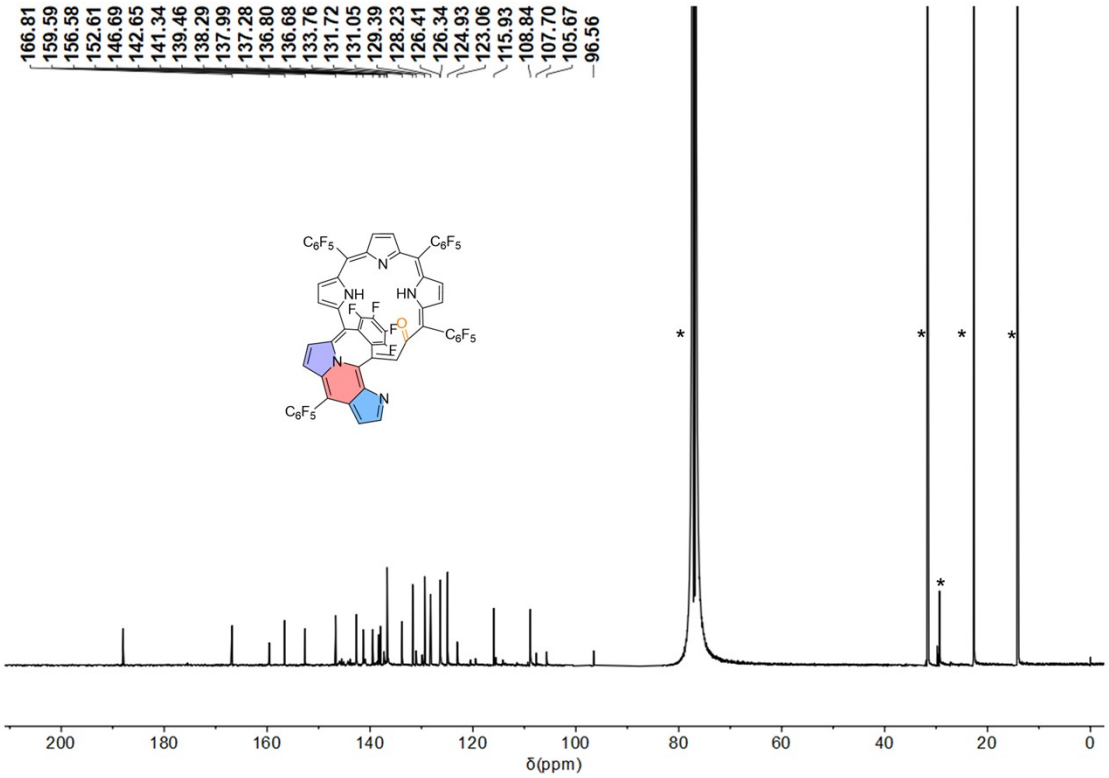

Figure S17. ^{13}C NMR (151 MHz) spectrum of **3** in $CDCl_3$.

4. HRMS Data

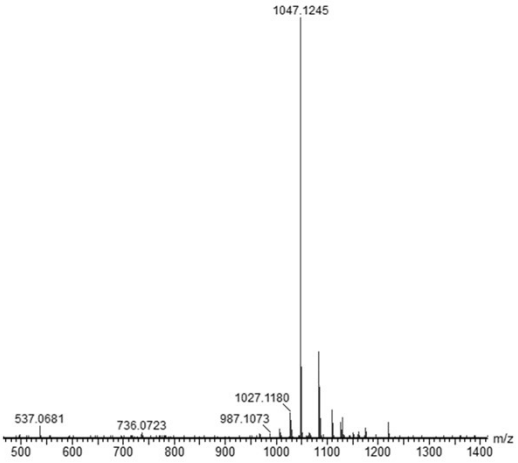

Figure S18. HRMS of **N-O-P$_4$** in CH_2Cl_2.

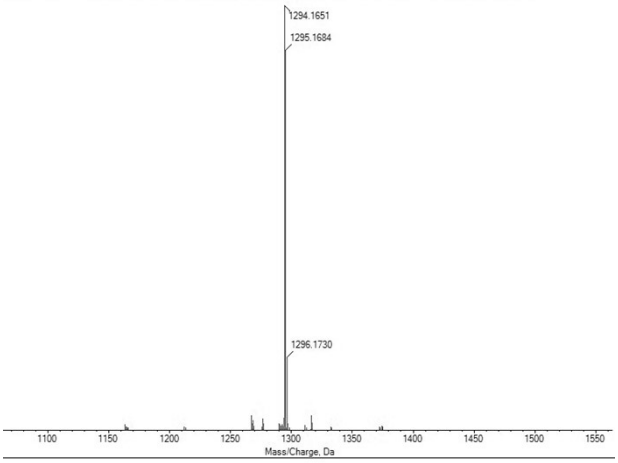

Figure S19. HRMS of **N-O-P$_5$** in CH_2Cl_2.

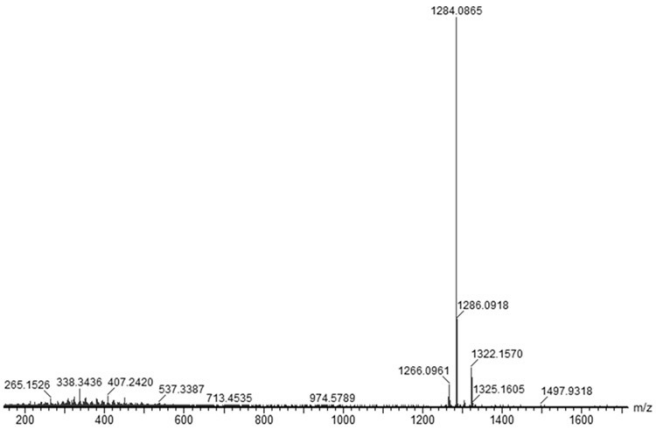

Figure S20. HRMS of **1** in CH_2Cl_2.

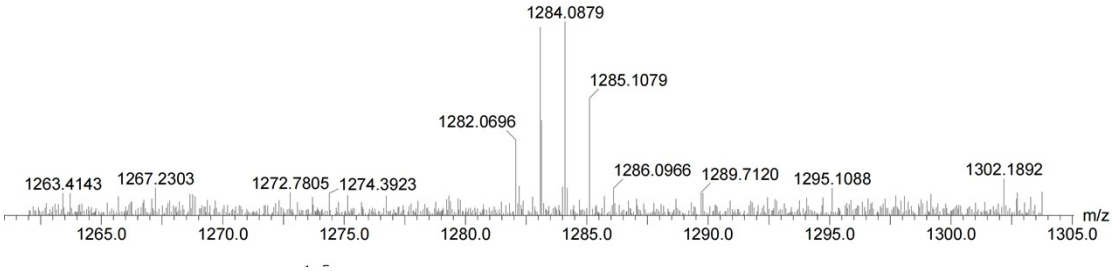

Figure S21. HRMS of **2** in CH_2Cl_2.

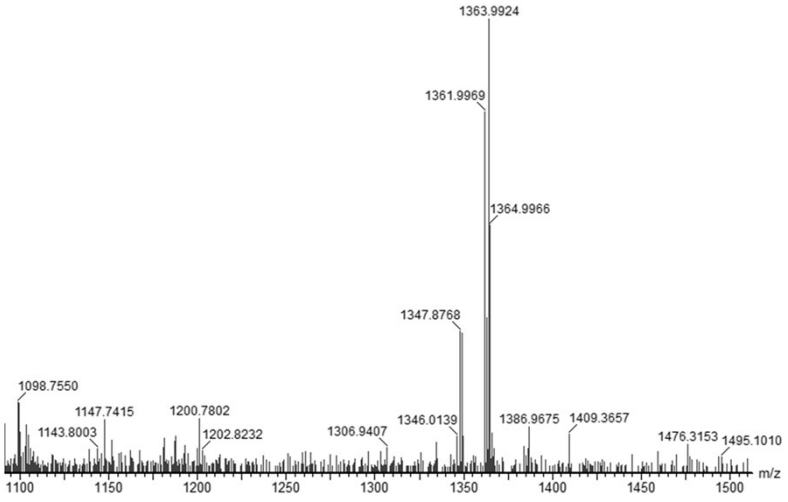

Figure S22. HRMS of **2-Br** in CH_2Cl_2.

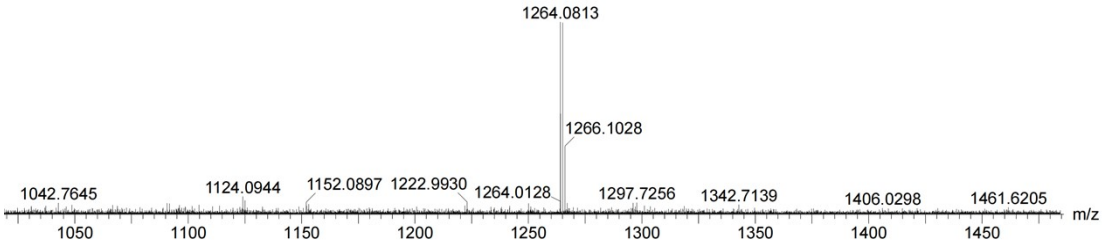

Figure S23. HRMS of **3** in CH_2Cl_2.

5. Plausible Mechanisms

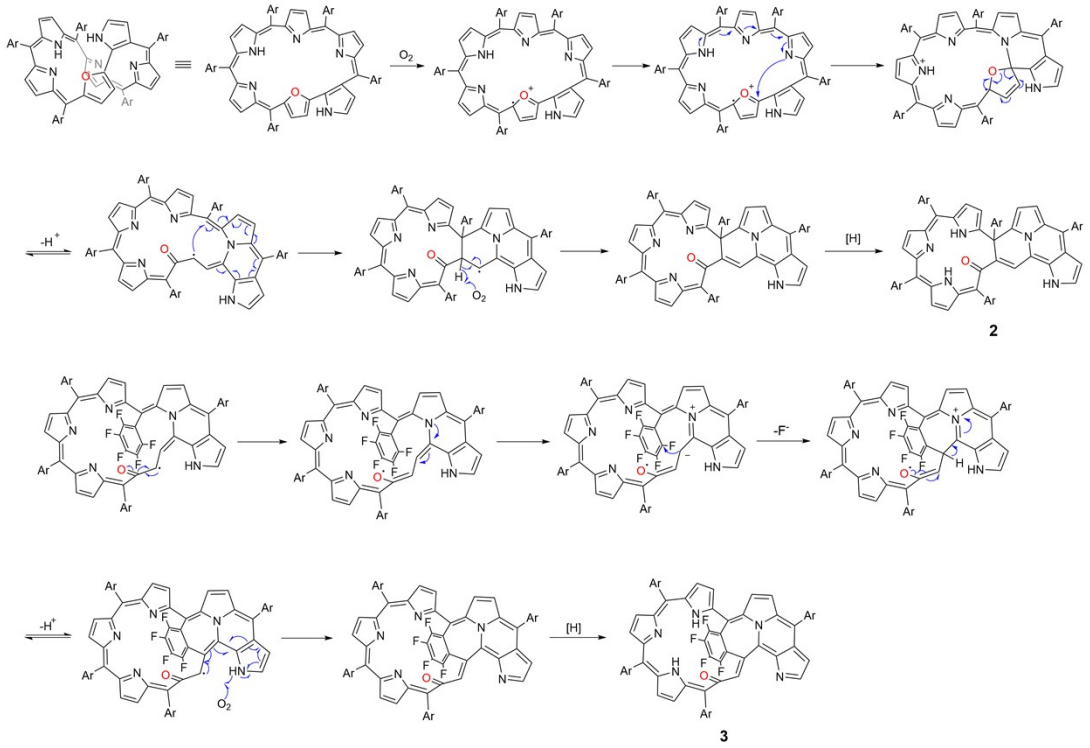

Figure S24. Plausible mechanisms proposed for the formation of compounds **2** and **3**.

6. Crystal Data

Table S2. Crystal data and structure refinements of **2-Br** and **3**.

Compounds	**2-Br**	**3**
Formula	$BrC_{59}F_{25}N_5O$	$C_{61}H_{17.5}Cl_{0.5}F_{24}N_5O$
Formula weight (g/mol)	1362.65	1310.02
Crystal system	orthorhombic	monoclinic
Temperature (K)	200.0	213.15
Crystal size (mm^3)	0.2×0.15×0.05	0.17×0.12×0.09
Theta range for data collection (°)	4.21–132.606	3.258–49.998
Space group	*Pba*2	*C*2/*c*
a (Å)	28.017(4)	42.207(4)
b (Å)	31.688(4)	27.543(3)
c (Å)	14.6695(18)	30.032(3)
α (°)	90	90
β (°)	90	132.753(2)
γ (°)	90	90
Volume ($Å^3$)	13024(3)	25636(4)
Z	8	16
ρ_{calc} (g/cm^3)	1.390	1.358
F (000)	5360.0	10416.0
μ (mm^{-1})	1.888	0.151
Index ranges	$-32 \le h \le 33$, $-37 \le k \le 37$, $-17 \le l \le 16$	$-50 \le h \le 50$, $-32 \le k \le 32$, $-35 \le l \le 35$
R_1 [$I > 2\sigma(I)$]	0.0680	0.0718
wR_2 (all data)	0.2181	0.2155
GOF	1.041	0.889
Largest diff. peak/hole (e $Å^{-3}$)	0.35/-0.56	0.34/-0.47
Reflections collected/Unique	174689/22222	148227/22559
CCDC number	2466477	2466476

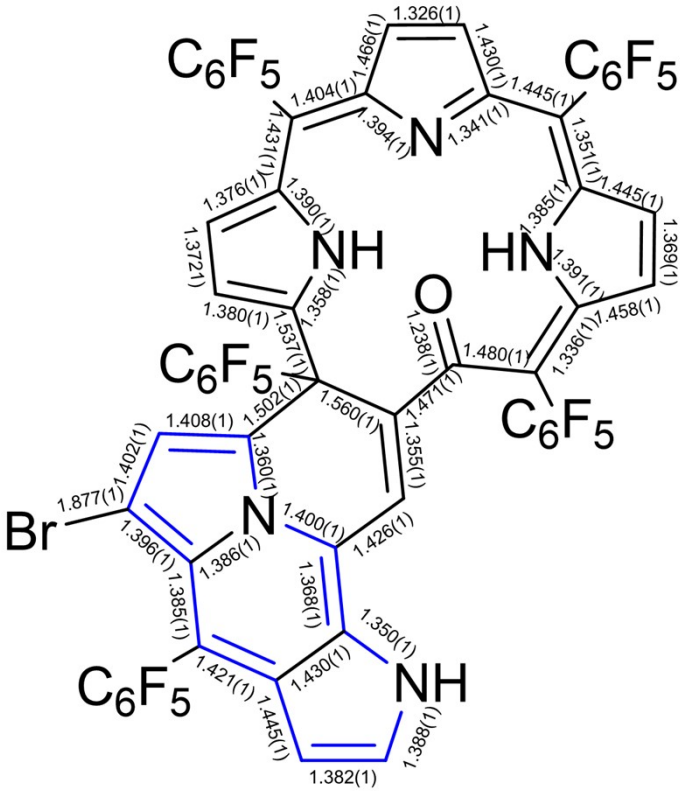

Figure S25. Selected bond lengths (Å) in the crystal structure of **2-Br** (based on the bonds along the circuit of ring current, the HOMA value of fused part was calculated to be 0.84).

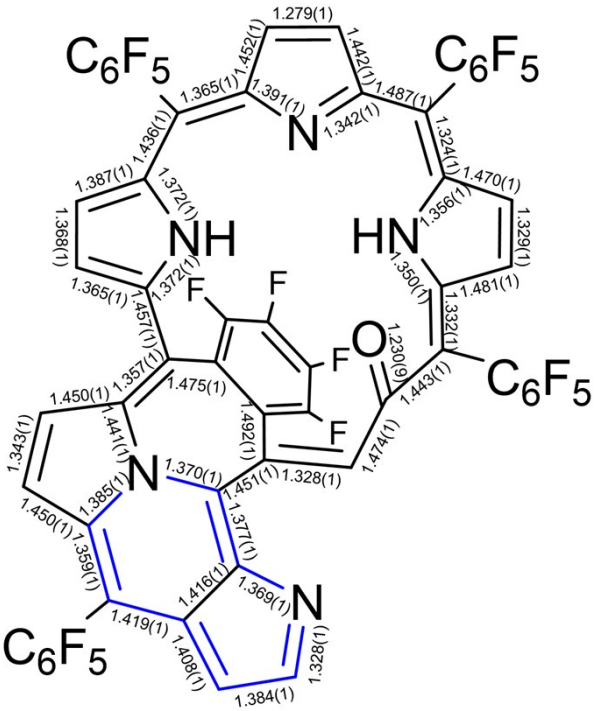

Figure S26. Selected bond lengths (Å) in the crystal structure of **3** (based on the bonds along the circuit of ring current, the HOMA value of fused part was calculated to be 0.89).

7. Electrochemical Data

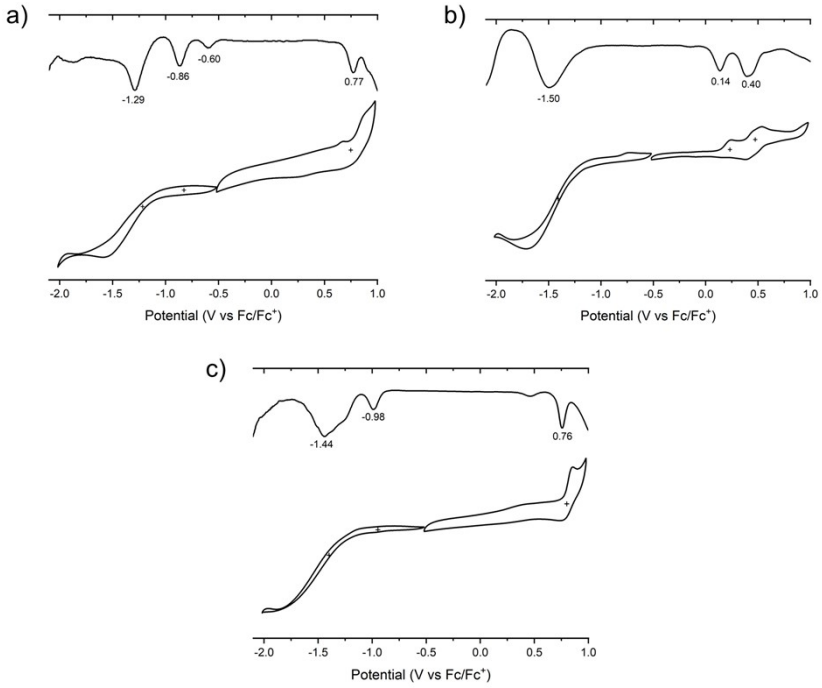

Figure S27. Cyclic voltammograms and differential pulse voltammograms of a) **1**, b) **2**, and c) **3** in CH_2Cl_2 containing 0.1 M $TBAPF_6$ at a scan rate of 0.10 V/s. The ferrocene/ferrocenium couple was used as an external reference.

Table S3. Electrochemical data for compounds **1**, **2**, and **3**.

Compounds	Oxidation(V)		Reduction (V)			Gap
	$E^{1/2}_{ox1}$	$E^{1/2}_{ox2}$	$E^{1/2}_{red1}$	$E^{1/2}_{red2}$	$E^{1/2}_{red3}$	(eV)
1	0.77	--	−0.60	−0.86	−1.29	1.37
2	0.14	0.40	−1.50	--	--	1.64
3	0.76	--	−0.98	−1.44	--	1.74

HOMO-LUMO energy gap = e ($E^{1/2}_{ox1}$ - $E^{1/2}_{red1}$). Oxidation and reduction potentials (V) were determined by differential pulse voltammograms (DPV) in DCM using 0.1 M $TBAPF_6$ as a supporting electrolyte and ferrocene as an external standard. (E_{Fc/Fc^+} = 0.53 V).

8. Chiral Resolution Data

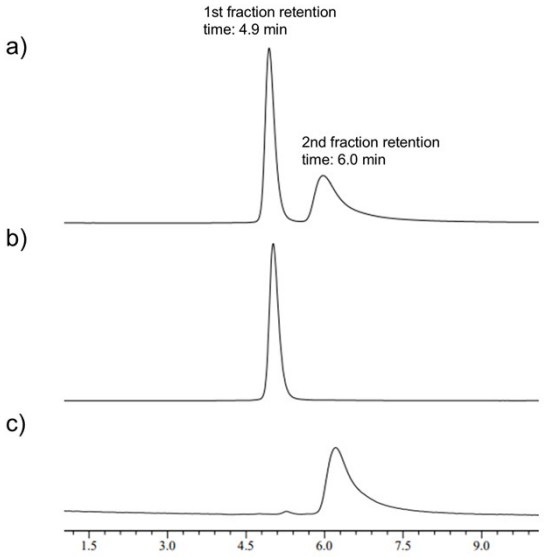

Figure S28. a) HPLC resolution of compound **2**. (Column: (DAICEL CHIRALPAK IA, φ 5 μm × 4.6 mm × 250 mm; mobile phase: n-hexane/ isopropanol = 4:1; flow rate: 0.8 mL/min). b) and c) HPLC traces of chiral isomer of compound **2** before the CD measurements.

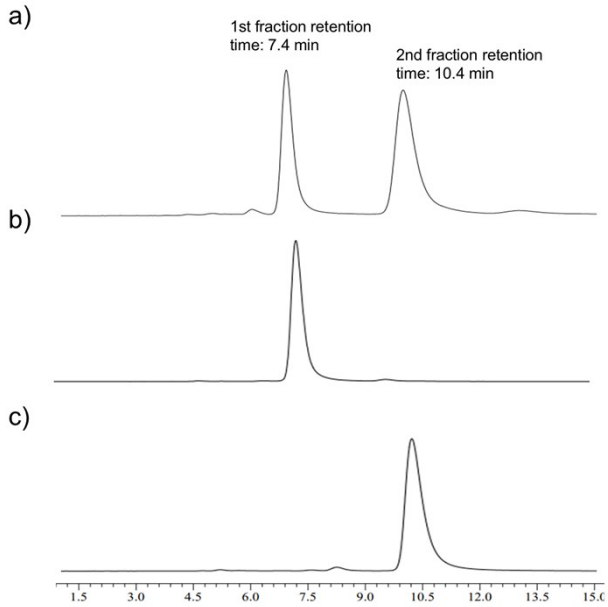

Figure S29. a) HPLC resolution of compound **3**. (Column: (DAICEL CHIRALPAK IA, φ 5 μm × 4.6 mm × 250 mm; mobile phase: n-hexane / isopropanol = 17:3; flow rate: 0.8 mL/min). b) and c) HPLC traces of chiral isomer of compound **3** before the CD measurements.

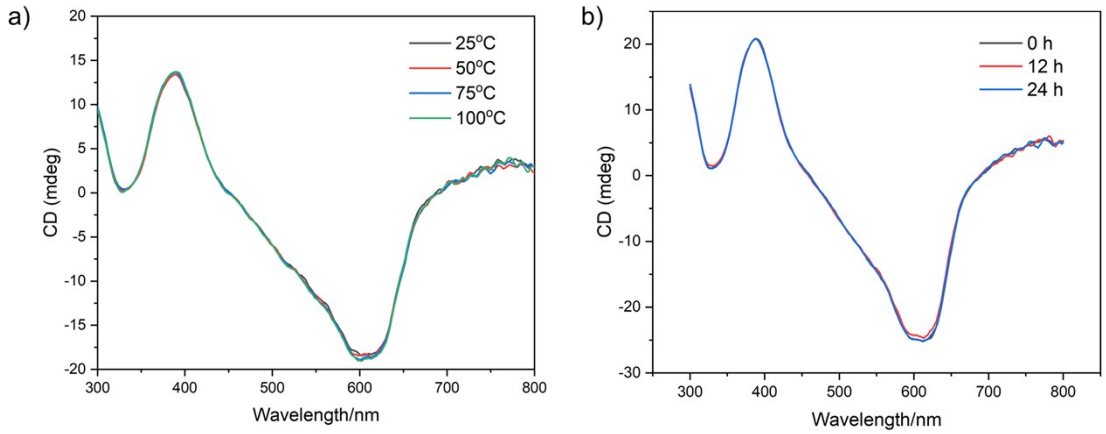

Figure S30. a) Temperature-dependent CD spectra of R enantiomer of **2** recorded in Toluene and b) Keeping R enantiomer of **2** at 100°C for 24 h.

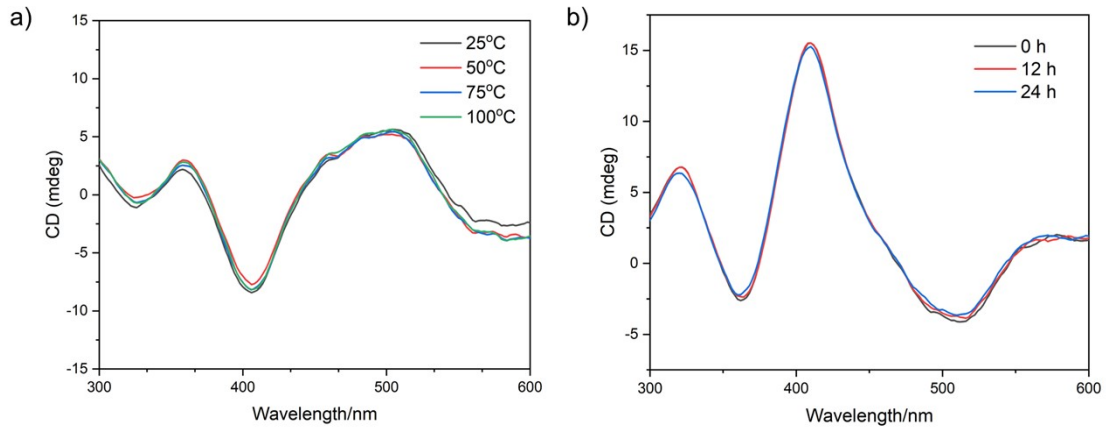

Figure S31. a) Temperature-dependent CD spectra of S_p enantiomer of **3** recorded in Toluene and b) Keeping R_p enantiomer of **3** at 100°C for 24 h.

9. DFT-Computational Data

Table S4. Calculated energy levels of the frontier molecular orbitals of compounds **1** – **3**.

Compounds	E_{HOMO} / eV	E_{LUMO} / eV	H-L gap / eV
1	−5.00	−3.22	1.78
2	−4.92	−3.07	1.85
3	−5.30	−3.41	1.89

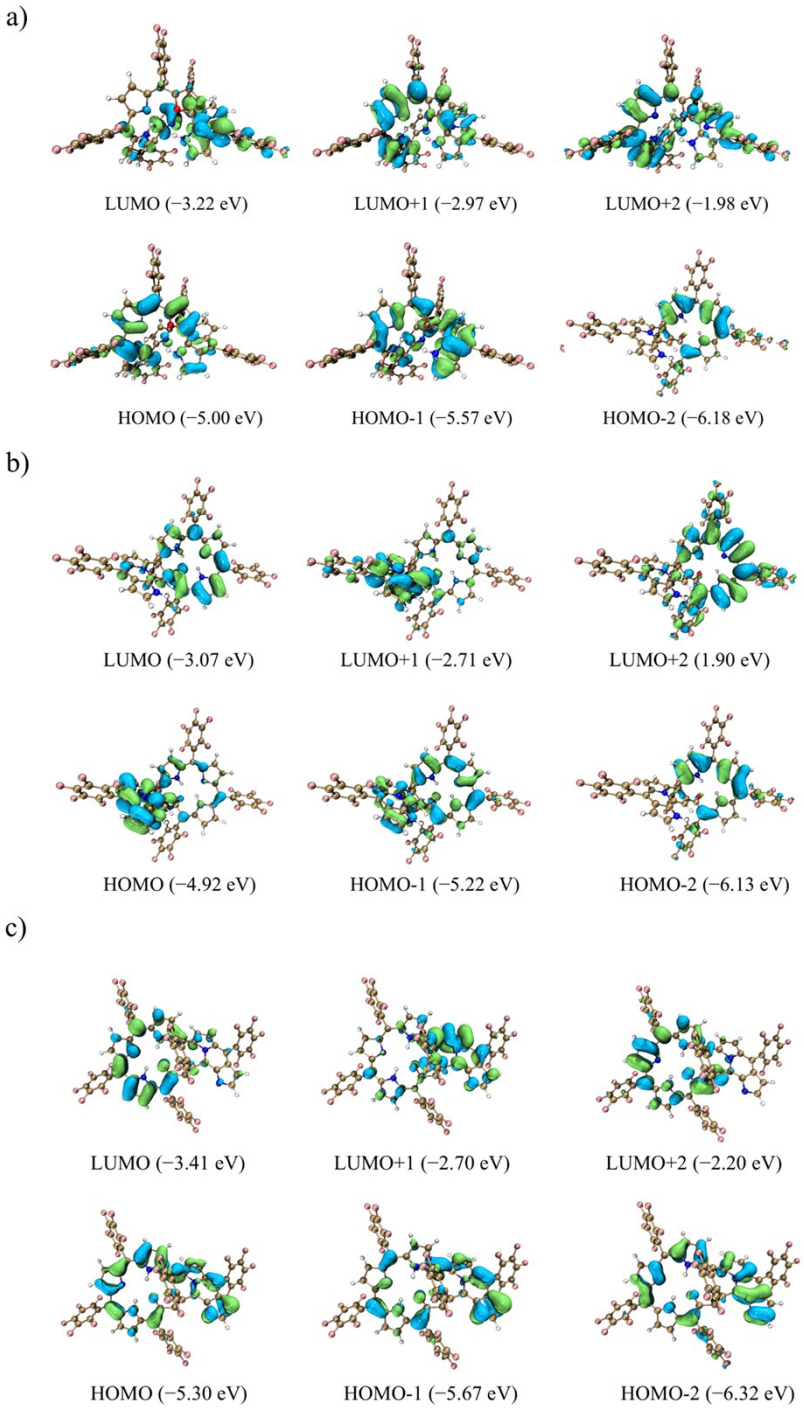

Figure S32. Contour plots of the molecular orbitals for compounds **1** – **3**.

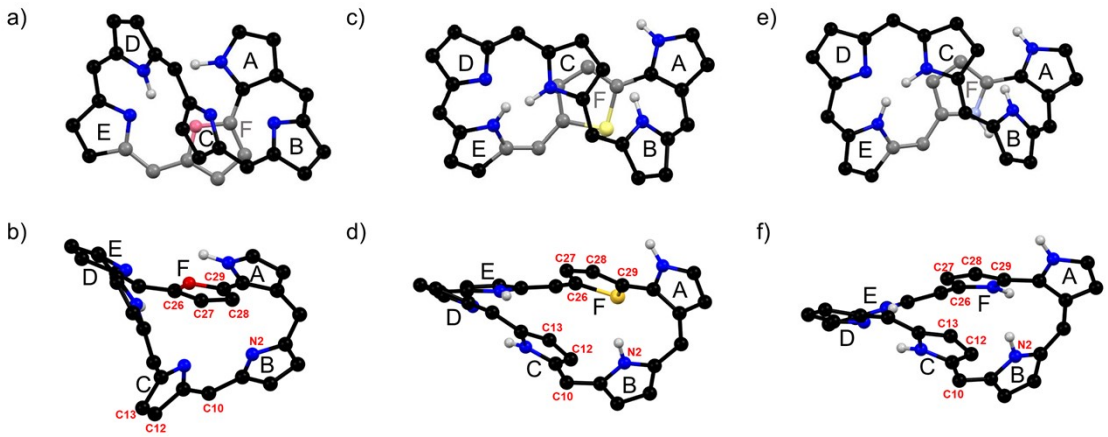

Figure S33. The optimized structures of compounds **1** (a, b), **S-Hex** (c, d)[S9a], and **N-Hex** (e, f)[S9b]. All C_6F_5 groups, and the hydrogen atoms attached to carbon atoms are omitted for clarity.

Table S5. Interplanar angles of rings A–F in the optimized structures of compounds **1**, **S-Hex**, and **N-Hex**.

Compounds	**1**	**S-Hex**	**N-Hex**
A-B	17.9°	34.8°	33.9°
B-C	17.6°	29.0°	22.6°
C-D	39.7°	24.5°	25.0°
D-E	89.7°	17.5°	19.3°
E-F	23.0°	48.1°	48.9°
F-A	37.6°	41.3°	35.5°

Table S6. Selected interatomic distances in the optimized structures of compounds **1**, **S-Hex**, and **N-Hex**.

Compounds	**1**	**S-Hex**	**N-Hex**
N2···C29	2.85	3.14	3.09
C10···C27	4.02	4.52	4.10
C10···C28	3.90	4.55	4.35
C12···C27	5.58	4.72	4.05
C12···C28	5.80	4.20	3.62
C13···C27	6.32	4.84	4.10
C13···C28	6.46	4.34	3.70

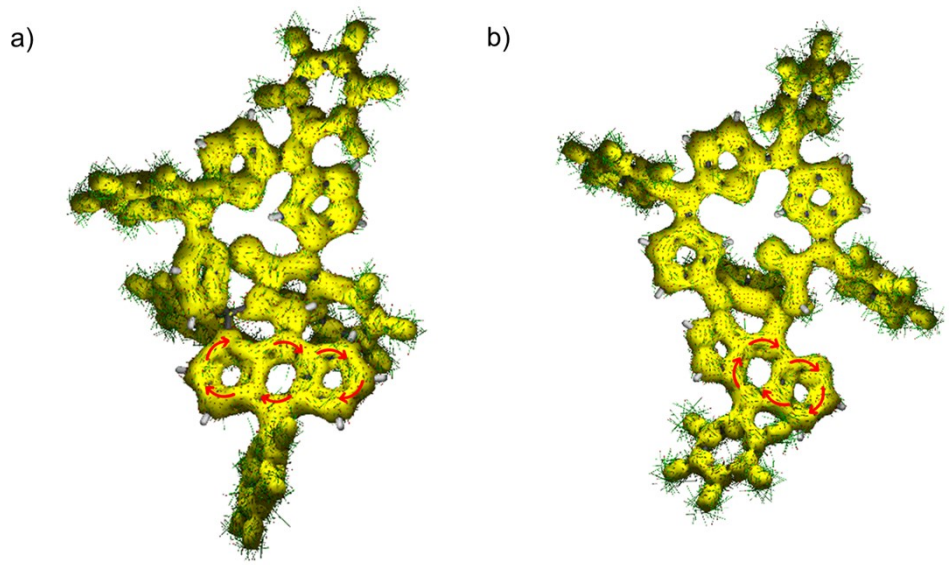

Figure S34. ACID plots of a) **2** and b) **3**. Direction of the applied magnetic field is perpendicular to the paper and pointing outward. The current density vectors indicate anticlockwise current. The isosurface value is 0.03.

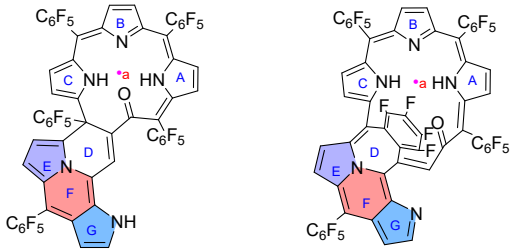

2 **3**

Table S7. NICS values of **2** and **3** based on its optimized structure (B3LYP/6-31G).

	Parameter	A	B	C	D	E	F	G	a
2	NICS(0)	−3.16	−3.00	−8.93	4.50	−15.4	−5.15	−9.85	0.24
	NICS(1)	−3.86	−5.82	−8.16	2.03	−12.6	−6.68	−8.40	--
	$NICS(1)_{zz}$	−5.14	−9.38	−16.1	4.40	−7.92	−4.19	−4.30	--
3	NICS(0)	−3.52	−3.08	−9.63	−0.04	−1.92	−5.66	−8.37	1.40
	NICS(1)	−4.57	−5.84	−8.34	−4.29	−3.02	−7.23	−10.8	--
	$NICS(1)_{zz}$	−6.61	−9.67	−19.1	5.67	−2.71	−10.8	−18.6	--

Table S8. Key parameters μ, m, and θ of **2** and **3** based on its optimized structure (B3LYP/6-31G).

Compound	λ/nm[a]	g_{abs}[a]	$\|\mu\|$ [$\times 10^{-18}$ esu cm][b]	$\|m\|$ [$\times 10^{-20}$ erg G^{-1}][b]	$\|\cos\theta\|$ [b]	$\|g_{abs}\|_{cald}$[b]
2	607	0.0021	3.94	2.23	0.165	0.0037
3	408	0.0009	4.89	0.44	0.591	0.0021

[a]Experimentally determined values. [b]Calculated by TD-DFT.

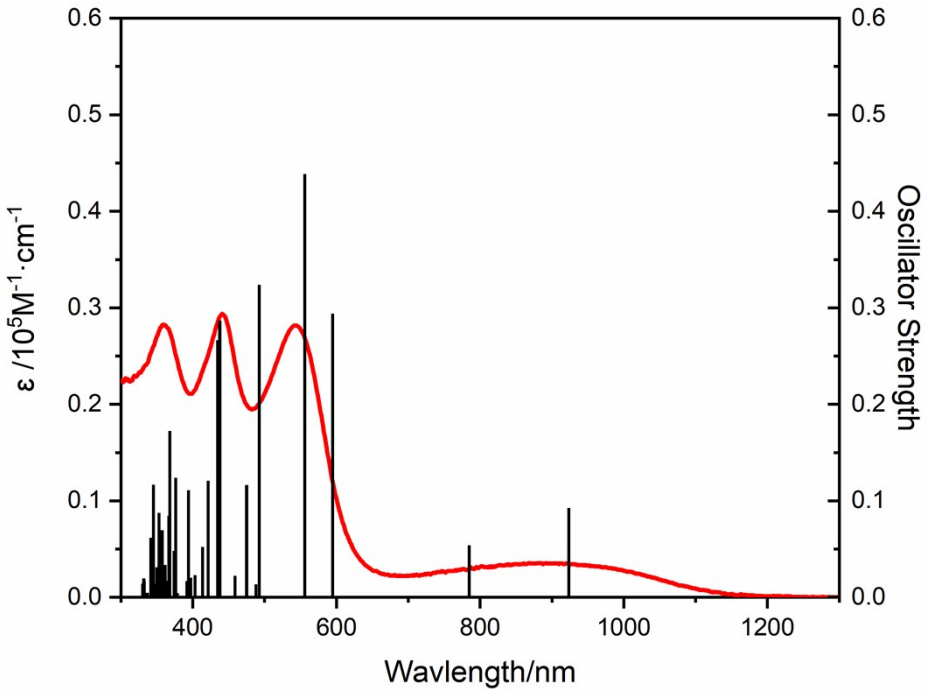

Figure S35. TD-DFT-computed vertical energies of **1** along with the experimental spectrum.

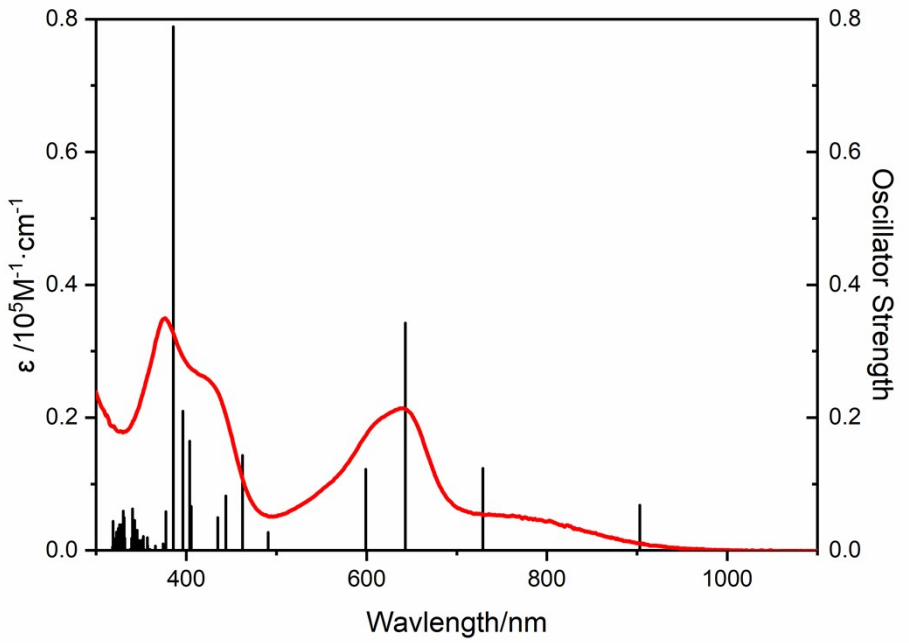

Figure S36. TD-DFT-computed vertical energies of **2** along with the experimental spectrum.

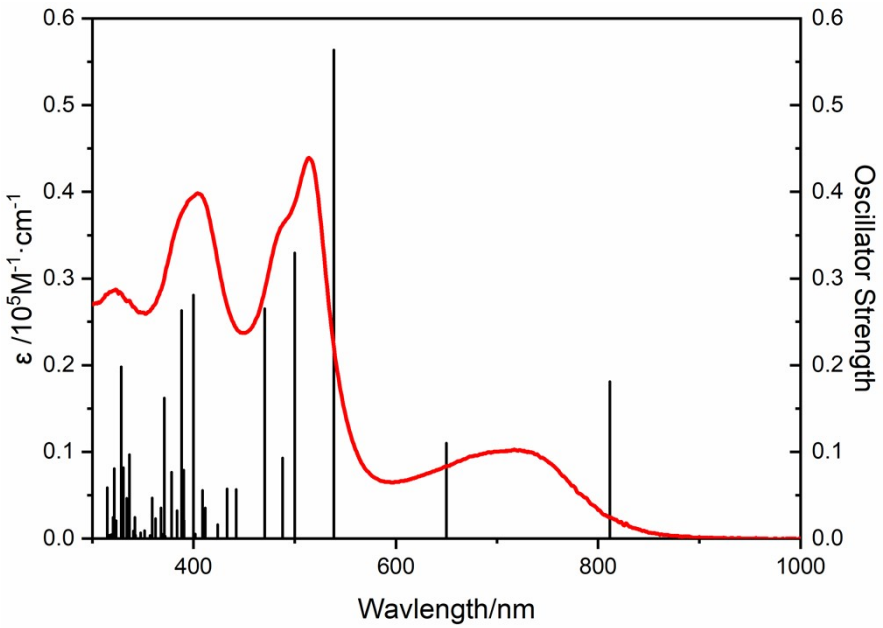

Figure S37. TD-DFT-computed vertical energies of **3** along with the experimental spectrum.

Table S9. Selected computed excitation energies, oscillator strengths and molecular orbital compositions for low-lying excited states of **1**.

	Wavelength	Oscillator strength	MO compositions
S1	923.5	0.0925	H→L (97%)
S2	784.7	0.0536	H-1→L (27%), H→L+1 (72%)
S3	594.8	0.2938	H-1→L (54%), H-1→L+1 (20%)
S4	556.0	0.4385	H-1→L (13%), H-1→L+1 (68%)
S5	492.6	0.3238	H-3→L (11%), H-2→L (60%), H→L+2 (11%)
S6	487.8	0.0132	H-3→L (67%), H-2→L (13%)
S7	475.0	0.1161	H-2→L (11%), H-2→L+1 (25%), H→L+2 (45%)
S8	458.7	0.022	H-2→L+1 (42%), H→L+3 (47%), H→L+2 (7%)
S9	437.7	0.2868	H-4→L (54%), H→L+3 (21%)
S10	434.6	0.2662	H-5→L (19%), H-4→L (15%), H→L+2 (15%), H→L+3 (14%)
S11	421.5	0.1207	H-10→L (12%), H-6→L (13%), H-5→L (25%), H-4→L (11%)
S12	413.6	0.0521	H-4→L+1 (10%), H-3→L+1 (75%)
S13	403.2	0.023	H-6→LUMO (44%), H-5→LUMO (27%) H-4→LUMO (10%)
S14	397.3	0.02	H-10→LUMO (13%), H-5→L+1 (16%), H-1→L+2 (47%)
S15	394.2	0.1107	H-6→L+1 (10%), H-4→L+1 (61%)

S16	391.7	0.0166	H-10→LUMO (15%), H-6→LUMO (19%), H-5→L+1 (31%)
S17	378.6	0.004	H-10→LUMO (21%), H-9→LUMO (73%)
S18	376.4	0.1237	H-6→L+1 (19%), H-5→L+1 (22%), H-1→L+2 (13%), H-1→L+3 (21%)
S19	375.5	0.0154	H-10→L (19%), H-7→L (48%)
S20	374.1	0.0479	H-7→L (22%), H-1→L+3 (43%)
S21	368.0	0.1724	H-12→L (30%), H-6→L+1 (28%)
S22	366.9	0.0843	H-12→L (65%), H-6→L+1 (11%)
S23	364.9	0.017	H-15→L (17%), H-15→L+1 (59%)
S24	362.8	0.0039	H-8→L (74%)
S25	362.2	0.0161	H-14→L (24%), H-11→L (41%), H-8→L (12%)
S26	361.6	0.0332	H-14→L (30%), H-11→L (40%)
S27	357.3	0.0693	H-13→L (50%)
S28	353.0	0.0874	H-10→L+1 (24%), H-9→L+1 (11%), H-7→L+1 (22%)
S29	350.1	0.031	H-16→L (31%), H-14→L (15%), H-13→L (24%)
S30	348.3	0.0141	H-15→L (23%), H-11→L+1 (32%), H-9→L+1 (14%), H-7→L+1 (15%)
S31	347.7	0.001	H-15→L (11%), H-10→L+1 (22%), H-7→L+1 (43%)
S32	347.4	0.0018	H-15→L (38%), H-15→L+1 (10%), H-11→L+1 (28%)
S33	346.3	0.0117	H-8→L+1 (81%)
S34	345.2	0.1167	H→L+4 (52%)
S35	341.6	0.0615	H-17→L (45%), H-16→L (10%), H→L+4 (22%)
S36	340.9	0.0013	H-11→L+1 (23%), H-10→L+1 (14%), H-9→L+1 (60%)
S37	336.8	0.0045	H-13→L+1 (67%), H→L+5 (10%)
S38	332.5	0.0166	H-2→L+2 (73%)
S39	331.7	0.0195	H→L+5 (45%)
S40	330.2	0.0139	H-18→L (31%)

Table S10. Selected computed excitation energies, oscillator strengths and molecular orbital compositions for low-lying excited states of **2**.

	Wavelength	Oscillator strength	MO compositions
S1	903.3	0.0683	H→L (99%)
S2	729.2	0.1233	H-1→L (46%), H→L+1 (52%)
S3	643.0	0.3424	H-1→L (47%), H→L+1 (46%)
S4	599.3	0.122	H-1→L+1 (90%), H-1→L (7%)
S5	490.9	0.0271	H-2→L (55%), H→L+2 (39%)
S6	462.4	0.1429	H-2→L (23%), H-1→L+2 (13%), H→L+2 (52%)
S7	443.9	0.0822	H-3→L (86%)
S8	435.0	0.0496	H-2→L+1 (62%), H-1→L+2 (32%)
S9	405.5	0.0664	H-6→L (28%), H-5→L (29%)
S10	404.0	0.1646	H-4→L (70%), H-1→L+2 (12%)
S11	396.3	0.2095	H-3→L+1 (76%)
S12	385.6	0.7885	H-4→L (14%), H-2→L (12%), H-2→L+1 (16%), H-1→L+2 (27%)
S13	377.6	0.0584	H->L+3 (92%)
S14	374.5	0.0098	H-6→L (38%), H-5→L (53%)
S15	365.9	0.0065	H-11→L (49%), H-8→L (34%)
S16	359.9	0.0016	H-7→L (97%)
S17	357.4	0.0074	H-11→L (28%), H-8→L (46%)
S18	356.9	0.0194	H-11→L (10%), H-9→L (56%)
S19	353.3	0.002	H-12→L (45%), H-6→L+1 (10%), H-5→L+1 (14%), H-4→L+1 (17%)
S20	352.4	0.0212	H-12→L (48%), H-6→L+1 (11%), H-5→L+1 (21%)
S21	351.2	0.0158	H-13→L (22%), H-4→L+1 (40%)
S22	348.1	0.015	H→L+4 (68%)
S23	345.6	0.0305	H-13→L (42%), H-4→L+1 (18%)
S24	342.9	0.0454	H-1→L+3 (72%)
S25	340.6	0.0627	H-14→L (65%), H-10→L (14%)
S26	339.6	0.0184	H-14→L (14%), H-10→L (48%), H-10→L+1 (11%), H-9→L (12%)
S27	337.8	0.0015	H-6→L+1 (50%), H-5→L+1 (36%)
S28	333.6	0.0005	H-17→L (13%), H-2→L+2 (10%), H→L+5 (41%)
S29	332.0	0.0184	H-20→L (11%), H-18→L (15%), H-16→L (39%)
S30	331.2	0.0493	H-18→L (11%), H-11→L+1 (14%), H→L+5 (20%)
S31	330.1	0.0593	H-2→L+2 (23%), H→L+6 (26%), H→L+7 (16%)

S32	328.6	0.0387	H-17→L (10%), H-9→L+1 (28%)
S33	327.1	0.0178	H-11→L+1 (37%), H-9→L+1 (12%)
S34	326.2	0.0387	H-2→L+2 (44%), H→L+5 (12%), H→L+6 (21%)
S35	324.9	0.0333	H-17→L (28%), H-15→L (22%)
S36	322.7	0.0278	H-12→L+1 (16%), H→L+7 (46%)
S37	320.5	0.0035	H→L+9 (68%)
S38	320.1	0.0178	H-12→L+1 (57%), H→L+7 (12%)
S39	319.0	0.0439	H-17→L (11%), H-15→L (48%)
S40	318.1	0.0054	H-12→L+1 (13%), H→L+8 (54%)

Table S11. Selected computed excitation energies, oscillator strengths and molecular orbital compositions for low-lying excited states of **3**.

	Wavelength	Oscillator strength	MO compositions
S1	811.6	0.1809	H→L (99%)
S2	649.9	0.1101	H-1→L (85%), H→L+1 (14%)
S3	538.7	0.5636	H-1→L (13%), H→L+1 (73%)
S4	499.9	0.3295	H-2→L (70%), H→L+2 (18%)
S5	488.0	0.0930	H-3→L (26%), H-1→L+1 (67%)
S6	470.4	0.2653	H-3→L (48%), H-1→L+1 (11%), H→L+2 (27%)
S7	442.3	0.0567	H-7→L (20%), H-4→L (29%), H→L+2 (17%)
S8	433.1	0.0575	H-4→L (48%), H-1→L+2 (10%), H→L+2 (14%)
S9	424.0	0.0161	H-7→L (18%), H-5→L (15%), H-4→L (15%), H-1→L+2 (25%), H→L+3 (12%)
S10	411.5	0.0354	H-7→L (23%), H-6→L (10%), H-5→L (50%)
S11	408.8	0.0556	H-2→L+1 (33%), H→L+3 (27%), H-5→L (9%), H-3→L (5%), H-3→L+1 (8%), H-1→L+3 (5%), H→L+2 (5%)
S12	401.6	0.0055	H-7→L (18%), H-6→L (78%)
S13	399.8	0.2812	H-2→L+1 (21%), H-1→L+2 (35%), H→L+3 (29%)
S14	390.6	0.0209	H-9→L (88%)
S15	390.2	0.0791	H-10→L (58%)
S16	388.3	0.2634	H-10→L (35%), H-3→L+1 (11%), H-1→L+2 (11%)
S17	383.7	0.0322	H-12→L (25%), H-11→L (42%)
S18	378.2	0.0767	H-3→L+1 (60%), H-2→L+1 (19%)
S19	371.9	0.0029	H-12→L (18%), H-8→L (68%)

S20	371.2	0.1621	H-13→L (10%), H-1→L+3 (24%), H→L+4 (45%)
S21	369.2	0.0049	H-12→L (26%), H-11→L (32%), H-8→L (22%)
S22	367.8	0.0353	H-13→L (74%)
S23	362.4	0.0233	H-15→L (54%), H-1→L+3 (10%)
S24	359.1	0.047	H-1→L+3 (47%), H→L+4 (30%)
S25	356.9	0.0036	H-20→L (16%), H-16→L (58%)
S26	351.7	0.0093	H-20→L (40%), H-18→L (16%), H-16→L (15%), H-14→L (18%)
S27	347.8	0.0067	H-16→L (17%), H-15→L (10%), H-14→L (52%)
S28	342.7	0.0038	H-20→L (16%), H-18→L (13%), H-17→L (51%)
S29	342.0	0.0244	H-7→L+1 (23%), H-4→L+1 (42%)
S30	340.5	0.0087	H-2→L+2 (60%)
S31	336.6	0.0968	H-7→L+1 (23%), H-5→L+1 (53%)
S32	334.0	0.0467	H-1→L+4 (70%)
S33	330.5	0.0818	H-7→L+1 (14%), H-5→L+1 (24%), H-4→L+1 (30%), H-2→L+2 (11%)
S34	328.7	0.198	H-18→L (23%), H-17→L (17%), H-2→L+2 (11%), H-1→L+4 (12%)
S35	323.4	0.0207	H-19→L (24%), H-6→L+1 (15%), H-3→L+2 (29%)
S36	321.6	0.0806	H-7→L+1 (10%), H-6→L+1 (26%), H-3→L+2 (41%)
S37	320.3	0.0244	H-19→L (12%), H-11→L+1 (22%), H-6→L+1 (34%)
S38	318.6	0.0045	H-19→L (14%), H-11→L+1 (16%), H-8→L+1 (34%)
S39	316.7	0.004	H-11→L+1 (33%), H-8→L+1 (52%)
S40	314.7	0.0587	H→L+5 (79%)

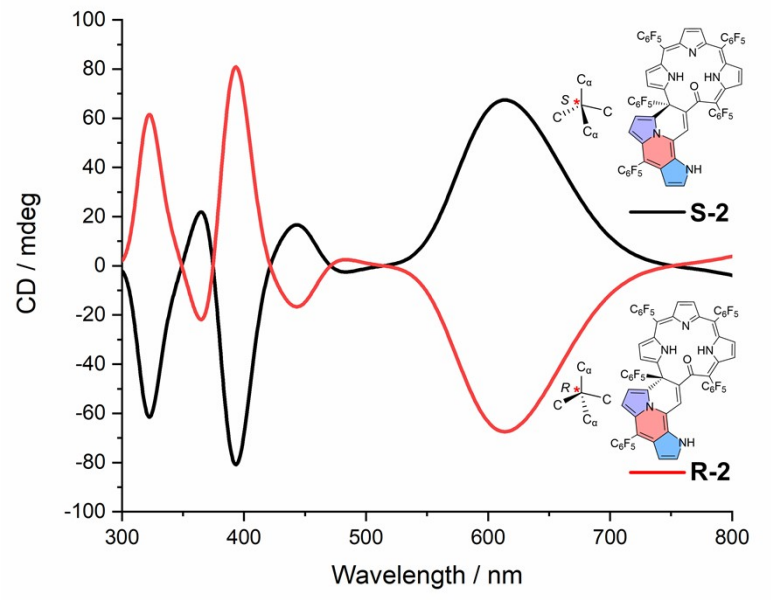

Figure S38. Simulated circular dichroism spectra of **R-2** and **S-2**.

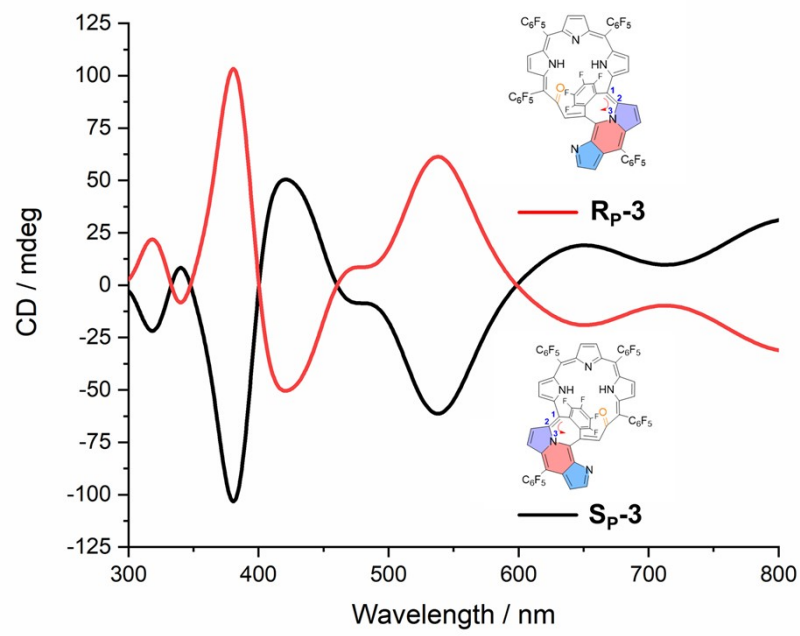

Figure S39. Simulated circular dichroism spectra of $\mathbf{S_p}$**-3** and $\mathbf{R_p}$**-3**.

Cartesian coordinates of the optimized structures for compounds 1–3.

Compound **1**

Row	Symbol	X	Y	Z
1	C	-0.512633000	0.453447000	3.537234000
2	C	0.499026000	-0.433636000	3.398717000
3	C	1.117726000	-0.141203000	2.095302000
4	N	0.340867000	0.795597000	1.401123000
5	O	0.027904000	-0.766545000	-1.865642000
6	C	1.240034000	-0.223483000	-2.144264000
7	C	2.217782000	-1.206132000	-2.079406000
8	C	1.564375000	-2.390395000	-1.714838000
9	C	-0.540338000	-4.298515000	-0.836197000
10	C	4.723946000	2.549698000	-2.911126000
11	C	-5.939315000	0.304600000	-1.700491000
12	C	3.033493000	-1.628443000	2.570383000
13	C	-1.744300000	3.201816000	3.094408000
14	C	-2.219459000	-2.491212000	-1.313132000
15	N	-2.535033000	-1.150299000	-1.337846000
16	C	-3.862989000	-1.072573000	-1.411734000
17	C	-4.465606000	-2.403679000	-1.496681000
18	C	-3.437018000	-3.290590000	-1.375170000
19	C	-0.901139000	-2.924749000	-1.281075000
20	C	0.306481000	3.062629000	-3.246113000
21	C	1.657178000	3.297230000	-3.150665000
22	C	2.261499000	2.128511000	-2.591030000
23	C	1.223082000	1.171455000	-2.442564000
24	N	0.057031000	1.777523000	-2.822802000
25	C	0.209551000	-2.094076000	-1.575516000
26	C	3.617998000	1.960929000	-2.137768000
27	C	-4.538466000	0.186641000	-1.238674000
28	C	-2.525115000	2.167160000	0.983197000
29	N	-2.694064000	1.135024000	0.079505000
30	C	-3.923424000	1.223387000	-0.545547000
31	C	-4.471604000	2.512226000	-0.160501000
32	C	-3.639362000	3.075945000	0.750765000
33	C	-1.617573000	2.190353000	2.016787000
34	C	2.400040000	-0.541553000	1.756329000
35	C	4.621979000	-0.335388000	0.432057000
36	C	5.028316000	0.476904000	-0.581153000
37	C	3.847223000	1.248997000	-0.959574000
38	N	2.806060000	0.987662000	-0.101643000
39	C	3.220048000	0.024467000	0.711024000
40	C	-0.594328000	1.172572000	2.255190000
41	C	0.103033000	-4.451883000	0.399353000

42	C	0.561759000	-5.686410000	0.843947000
43	C	0.335677000	-6.819739000	0.063848000
44	C	-0.335432000	-6.704275000	-1.152633000
45	C	-0.759109000	-5.450463000	-1.591199000
46	C	-6.270861000	0.014560000	-3.032826000
47	C	-7.578892000	0.068005000	-3.504588000
48	C	-8.609108000	0.421235000	-2.635275000
49	C	-8.319935000	0.710120000	-1.303693000
50	C	-7.004904000	0.635892000	-0.851199000
51	C	-0.633713000	3.973977000	3.471150000
52	C	-0.689601000	4.896552000	4.511907000
53	C	-1.878929000	5.066414000	5.217774000
54	C	-2.998720000	4.309558000	4.879849000
55	C	-2.917737000	3.386078000	3.841119000
56	C	3.228202000	-2.902210000	2.028376000
57	C	3.769827000	-3.951792000	2.763108000
58	C	4.162265000	-3.732377000	4.081455000
59	C	4.009923000	-2.467514000	4.645409000
60	C	3.460462000	-1.435239000	3.887060000
61	C	5.798129000	3.212024000	-2.288788000
62	C	6.833167000	3.789983000	-3.017513000
63	C	6.822812000	3.719715000	-4.409148000
64	C	5.775412000	3.071926000	-5.061330000
65	C	4.748508000	2.500726000	-4.317083000
66	F	0.755338000	-8.015261000	0.483427000
67	F	-0.555307000	-7.793241000	-1.897491000
68	F	-1.385791000	-5.366940000	-2.773413000
69	F	1.198592000	-5.790077000	2.016472000
70	F	0.298903000	-3.384843000	1.187299000
71	F	3.782002000	1.864191000	-4.989240000
72	F	5.770899000	2.990665000	-6.395910000
73	F	7.812632000	4.268069000	-5.114219000
74	F	7.830533000	4.422647000	-2.391390000
75	F	5.842382000	3.333854000	-0.957512000
76	F	3.325739000	-0.234494000	4.465963000
77	F	2.898634000	-3.147759000	0.749144000
78	F	3.917317000	-5.159912000	2.208432000
79	F	4.685724000	-4.728265000	4.800308000
80	F	4.394916000	-2.250169000	5.907906000
81	F	-5.305080000	-0.318052000	-3.901135000
82	F	-7.851556000	-0.204368000	-4.785876000
83	F	-9.867840000	0.483110000	-3.077019000
84	F	-9.308895000	1.032782000	-0.461864000
85	F	-6.782147000	0.883941000	0.448209000

86	F	0.520418000	3.845008000	2.809314000
87	F	0.384204000	5.627020000	4.831738000
88	F	-1.945907000	5.951974000	6.214784000
89	F	-4.136260000	4.457059000	5.569761000
90	F	-4.007647000	2.647858000	3.581942000
91	H	-1.180992000	0.585516000	4.378673000
92	H	0.842019000	-1.157982000	4.123286000
93	H	3.274198000	-1.064984000	-2.246687000
94	H	2.014968000	-3.358000000	-1.558511000
95	H	-5.522128000	-2.620184000	-1.588143000
96	H	-3.487104000	-4.371223000	-1.390950000
97	H	-0.499719000	3.707459000	-3.563634000
98	H	2.162712000	4.226635000	-3.370904000
99	H	-0.843572000	1.317617000	-2.775818000
100	H	-5.406280000	2.911174000	-0.526956000
101	H	-3.771500000	4.017755000	1.263207000
102	H	5.209134000	-1.080554000	0.953209000
103	H	5.990507000	0.494710000	-1.076043000
104	H	-2.091769000	0.323484000	-0.054179000

Compound **2**

Row	Symbol	X	Y	Z
1	C	2.676853000	-0.598682000	-1.061460000
2	N	3.298369000	0.319337000	-0.226923000
3	C	2.801439000	0.770291000	0.961815000
4	C	3.772441000	1.594110000	1.534261000
5	H	3.662336000	2.103364000	2.482052000
6	C	4.874464000	1.657972000	0.670004000
7	C	4.590753000	0.850280000	-0.443206000
8	C	5.282095000	0.498266000	-1.626452000
9	C	4.664501000	-0.374448000	-2.527579000
10	C	3.371922000	-0.919713000	-2.220195000
11	N	3.040249000	-1.787802000	-3.231498000
12	H	2.197224000	-2.339579000	-3.278824000
13	C	4.070007000	-1.810996000	-4.165797000
14	H	3.990937000	-2.437968000	-5.042407000
15	C	5.068027000	-0.966233000	-3.777972000
16	H	5.985649000	-0.776551000	-4.313450000
17	C	6.631995000	1.045017000	-1.885659000
18	C	6.929809000	1.713464000	-3.081047000
19	F	5.978698000	1.882571000	-4.010957000
20	C	8.195422000	2.227613000	-3.348079000
21	F	8.438852000	2.864407000	-4.498485000

22	C	9.209041000	2.086985000	-2.402720000
23	C	8.947983000	1.428782000	-1.202937000
24	C	7.676993000	0.914479000	-0.960523000
25	F	7.477719000	0.266314000	0.194510000
26	F	9.921453000	1.279929000	-0.298725000
27	F	10.425282000	2.578473000	-2.646508000
28	C	1.395910000	0.138535000	2.891231000
29	C	0.755399000	0.882073000	3.884130000
30	F	0.052776000	1.986710000	3.593066000
31	C	0.795171000	0.508528000	5.228021000
32	F	0.162519000	1.248297000	6.145996000
33	C	1.491560000	-0.630341000	5.617237000
34	F	1.528539000	-0.992364000	6.902307000
35	C	2.150170000	-1.389534000	4.653830000
36	C	2.109181000	-0.986481000	3.325370000
37	F	2.772802000	-1.749804000	2.435296000
38	F	2.826053000	-2.487960000	5.006375000
39	C	0.846013000	2.891199000	0.525955000
40	C	-0.332382000	3.594963000	0.246495000
41	H	-0.409894000	4.599191000	-0.145294000
42	H	1.859474000	3.246381000	0.416417000
43	H	5.786904000	2.214810000	0.819280000
44	C	2.676853000	-0.598682000	-1.061460000
45	N	3.298369000	0.319337000	-0.226923000
46	C	2.801439000	0.770291000	0.961815000
47	C	3.772441000	1.594110000	1.534261000
48	H	3.662336000	2.103364000	2.482052000
49	C	4.874464000	1.657972000	0.670004000
50	C	4.590753000	0.850280000	-0.443206000
51	C	5.282095000	0.498266000	-1.626452000
52	C	4.664501000	-0.374448000	-2.527579000
53	C	3.371922000	-0.919713000	-2.220195000
54	N	3.040249000	-1.787802000	-3.231498000
55	H	2.197224000	-2.339579000	-3.278824000
56	C	4.070007000	-1.810996000	-4.165797000
57	H	3.990937000	-2.437968000	-5.042407000
58	C	5.068027000	-0.966233000	-3.777972000
59	H	5.985649000	-0.776551000	-4.313450000
60	C	6.631995000	1.045017000	-1.885659000
61	C	6.929809000	1.713464000	-3.081047000
62	F	5.978698000	1.882571000	-4.010957000
63	C	8.195422000	2.227613000	-3.348079000
64	F	8.438852000	2.864407000	-4.498485000
65	C	9.209041000	2.086985000	-2.402720000

66	C	8.947983000	1.428782000	-1.202937000
67	C	7.676993000	0.914479000	-0.960523000
68	F	7.477719000	0.266314000	0.194510000
69	F	9.921453000	1.279929000	-0.298725000
70	F	10.425282000	2.578473000	-2.646508000
71	C	1.395910000	0.138535000	2.891231000
72	C	0.755399000	0.882073000	3.884130000
73	F	0.052776000	1.986710000	3.593066000
74	C	0.795171000	0.508528000	5.228021000
75	F	0.162519000	1.248297000	6.145996000
76	C	1.491560000	-0.630341000	5.617237000
77	F	1.528539000	-0.992364000	6.902307000
78	C	2.150170000	-1.389534000	4.653830000
79	C	2.109181000	-0.986481000	3.325370000
80	F	2.772802000	-1.749804000	2.435296000
81	F	2.826053000	-2.487960000	5.006375000
82	C	0.846013000	2.891199000	0.525955000
83	C	-0.332382000	3.594963000	0.246495000
84	H	-0.409894000	4.599191000	-0.145294000
85	H	1.859474000	3.246381000	0.416417000
86	H	5.786904000	2.214810000	0.819280000
87	C	2.676853000	-0.598682000	-1.061460000
88	N	3.298369000	0.319337000	-0.226923000
89	C	2.801439000	0.770291000	0.961815000
90	C	3.772441000	1.594110000	1.534261000
91	H	3.662336000	2.103364000	2.482052000
92	C	4.874464000	1.657972000	0.670004000
93	C	4.590753000	0.850280000	-0.443206000
94	C	5.282095000	0.498266000	-1.626452000
95	C	4.664501000	-0.374448000	-2.527579000
96	C	3.371922000	-0.919713000	-2.220195000
97	N	3.040249000	-1.787802000	-3.231498000
98	H	2.197224000	-2.339579000	-3.278824000
99	C	4.070007000	-1.810996000	-4.165797000
100	H	3.990937000	-2.437968000	-5.042407000
101	C	5.068027000	-0.966233000	-3.777972000
102	H	5.985649000	-0.776551000	-4.313450000
103	C	6.631995000	1.045017000	-1.885659000
104	C	6.929809000	1.713464000	-3.081047000

Compound **3**

Row	Symbol	X	Y	Z
1	C	0.459737000	2.613495000	0.277550000

2	C	0.412422000	3.972845000	-0.067294000
3	H	1.258439000	4.644233000	-0.071478000
4	C	-0.923083000	4.303871000	-0.271194000
5	H	-1.313325000	5.276587000	-0.530609000
6	C	-1.704936000	3.142526000	-0.070333000
7	C	-3.124491000	3.069524000	-0.149573000
8	C	-3.974114000	1.965201000	-0.155011000
9	C	-5.426889000	2.092341000	-0.146040000
10	H	-5.984587000	3.013691000	-0.059185000
11	C	-5.923325000	0.836417000	-0.246135000
12	H	-6.961562000	0.536557000	-0.259394000
13	C	-4.770244000	-0.052030000	-0.320714000
14	C	-4.901012000	-1.480046000	-0.500785000
15	C	-3.850434000	-2.370657000	-0.481799000
16	C	-3.850908000	-3.806760000	-0.701525000
17	H	-4.730035000	-4.389933000	-0.934273000
18	C	-2.574757000	-4.255081000	-0.576354000
19	H	-2.219744000	-5.269979000	-0.677904000
20	C	-1.722807000	-3.115811000	-0.268856000
21	C	-0.348117000	-3.075951000	-0.052926000
22	C	0.276897000	-1.818774000	0.286734000
23	C	1.768485000	-1.718813000	0.268080000
24	H	2.299784000	-2.218441000	-0.538399000
25	C	2.443013000	-0.915329000	1.099964000
26	C	3.798000000	-0.445756000	0.765866000
27	C	4.958721000	-1.173306000	0.793513000
28	C	6.208435000	-0.626358000	0.263717000
29	C	7.144500000	-1.634376000	0.467139000
30	H	8.189367000	-1.636020000	0.188833000
31	C	6.420198000	-2.699907000	1.078934000
32	H	6.838967000	-3.656349000	1.378152000
33	N	5.121438000	-2.449440000	1.272681000
34	C	6.187342000	0.639618000	-0.381609000
35	C	4.987080000	1.332073000	-0.397064000
36	C	4.551237000	2.474566000	-1.158857000
37	H	5.203510000	3.055917000	-1.794950000
38	C	3.216831000	2.654798000	-0.975500000
39	H	2.600046000	3.420073000	-1.419870000
40	C	2.745439000	1.718596000	0.025972000
41	C	1.565091000	1.771921000	0.739301000
42	C	1.352265000	1.090201000	2.027383000
43	C	0.706101000	1.738592000	3.090992000
44	C	0.534930000	1.111942000	4.322283000
45	C	1.019106000	-0.177832000	4.524400000

46	C	1.663443000	-0.836386000	3.478629000
47	C	1.817316000	-0.218319000	2.244422000
48	F	2.111603000	-2.079525000	3.683293000
49	F	0.855317000	-0.774925000	5.707019000
50	F	-0.075194000	1.756860000	5.321558000
51	F	0.243231000	2.992875000	2.972871000
52	N	3.854070000	0.850364000	0.276888000
53	C	7.380316000	1.202613000	-1.053542000
54	C	8.124963000	0.462020000	-1.981857000
55	C	9.272046000	0.971376000	-2.585013000
56	C	9.701095000	2.260227000	-2.275917000
57	C	8.979673000	3.027858000	-1.364382000
58	C	7.841222000	2.495015000	-0.766491000
59	F	7.180760000	3.264906000	0.112281000
60	F	9.388204000	4.264929000	-1.061910000
61	F	10.794573000	2.759735000	-2.855154000
62	F	9.952864000	0.237209000	-3.471109000
63	F	7.735000000	-0.770728000	-2.329589000
64	O	-0.376517000	-0.776090000	0.506311000
65	C	0.480461000	-4.295748000	-0.160640000
66	C	0.540625000	-5.061415000	-1.332797000
67	C	1.355835000	-6.183446000	-1.444315000
68	C	2.157954000	-6.559988000	-0.368204000
69	C	2.127266000	-5.821870000	0.813352000
70	C	1.288973000	-4.714581000	0.906776000
71	F	1.258069000	-4.043873000	2.064670000
72	F	2.880401000	-6.194776000	1.850584000
73	F	2.948183000	-7.631334000	-0.468314000
74	F	1.386780000	-6.891222000	-2.579858000
75	F	-0.206535000	-4.716480000	-2.394877000
76	N	-2.543620000	-2.024431000	-0.229704000
77	H	-2.229429000	-1.077595000	-0.032196000
78	C	-6.263235000	-2.033735000	-0.734518000
79	C	-7.008524000	-1.682326000	-1.866606000
80	C	-8.286945000	-2.183422000	-2.094981000
81	C	-8.132304000	-3.448936000	-0.047455000
82	C	-8.849426000	-3.073226000	-1.181153000
83	C	-6.858583000	-2.926126000	0.164306000
84	F	-6.199139000	-3.306659000	1.267649000
85	F	-10.071367000	-3.565728000	-1.393380000
86	F	-8.671161000	-4.300502000	0.831537000
87	F	-8.971301000	-1.828161000	-3.187211000
88	F	-6.492041000	-0.835149000	-2.765670000
89	N	-3.610179000	0.627491000	-0.234770000

90	C	-3.784252000	4.410518000	-0.250972000
91	C	-3.792812000	5.294789000	0.832092000
92	C	-4.396127000	6.547332000	0.752627000
93	C	-5.007037000	6.940245000	-0.437108000
94	C	-5.011354000	6.081432000	-1.534505000
95	C	-4.402392000	4.832754000	-1.431297000
96	F	-4.420103000	4.030279000	-2.502050000
97	F	-5.593952000	6.461101000	-2.676553000
98	F	-5.588052000	8.138362000	-0.524791000
99	F	-4.395909000	7.370688000	1.805986000
100	F	-3.213481000	4.942121000	1.985677000
101	N	-0.822227000	2.131488000	0.261281000
102	H	-1.059863000	1.151299000	0.397965000

10. References

[S1] G. M. Sheldrick, SHELXS97 and SHELXL97 Programs for Crystal Structure Solution and Refinement, University of Göttigen, Germany, **1997**.

[S2] a) O. V. Dolomanov, L. J. Bourhis, R. J. Gildea, J. A. K. Howard and H. Puschmann, OLEX2: a complete structure solution, refinement and analysis program. *J. Appl. Cryst.* **2009**, *42*, 339–341.; b) G.M. Sheldrick, A short history of SHELX. *Acta Cryst.* **2008**, *64*, 112–122.

[S3] G. M. Sheldrick, Crystal structure refinement with SHELXL. *Acta Crystallogr. Sect. C* **2015**, *71*, 3–8.

[S4] G. A. Petersson, A. Bennett, T. G. Tensfeldt. M. A. Al-Laham, W. A. Shirley and J. Mantzaris, A complete basis set model chemistry. I. The total energies of closed-shell atoms and hydrides of the first-row elements. *J. Chem. Phys.* **1988**, *89*, 2193–2218.

[S5] G. A. Petersson and M. A. Al-Laham, A complete basis set model chemistry. II. Open-shell systems and the total energies of the first-row atoms. *J. Chem. Phys.* **1991**, *94*, 6081–6090.

[S6] Z. Chen, C. S. Wannere, C. Corminboeuf, R. Puchta, and P. von R. Schleyer, Nucleus-Independent Chemical Shifts (NICS) as an Aromaticity Criterion. *Chem. Rev.* **2005**, *105*, 3842–3888.

[S7] P. von R. Schleyer, C. Maerker, A. Dransfeld, H. Jiao and N. J. R. v. E. Hommes, Nucleus-Independent Chemical Shifts: A Simple and Efficient Aromaticity Probe. *J. Am. Chem. Soc.* **1996**, *118*, 6317–6318.

[S8] a) T. A. Keith and R. F. W. Bader, Calculation of magnetic response properties using a continuous set of gauge transformations. *Chem. Phys. Lett.* **1993**, *210*, 223–231; b) J. P. Perdew, K. Burke and M. Ernzerhof, Generalized Gradient Approximation Made Simple. *Phys. Rev. Lett.* **1996**, *77*, 3865.

[S9] a) Q. Li, M. Ishida, H. Kai, T. Gu, C. Li, X. Li, G. Baryshnikov, X. Liang, W. Zhu, H. Ågren, H. Furuta and Y. Xie, Skeletal Rearrangement of Twisted Thia-Norhexaphyrin: Multiply Annulated Polypyrrolic Aromatic Macrocycles, *Angew. Chem. Int. Ed.*, 2019, **58**, 5925–5929; b) M. Li, B. Zhu, S. Li, R. Yu, G. Baryshnikov, C. Li, F. Sha, X. Wu, H. Ågren, Y. Xie and Q. Li, Pd(II) and Cu(III) Complexes of Multiply Fused Pentaphyrin Isomers with Tunable Structures and NIR Absorption, *Inorg. Chem.*, 2024, **63**, 13392–13401.